

Quantum geometry and bounds on dissipation in slowly driven quantum systems

Iliya Esin,^{1,2} Étienne Lantagne-Hurtubise,^{1,3} Frederik Nathan,^{1,4} and Gil Refael¹

¹Department of Physics and Institute for Quantum Information and Matter, California Institute of Technology, Pasadena, California 91125, USA

²Department of Physics, Bar-Ilan University, 52900, Ramat Gan, Israel

³Département de Physique and Institut Quantique,

Université de Sherbrooke, Sherbrooke, Québec, Canada J1K 2R1

⁴Center for Quantum Devices and NNF Quantum Computing Programme, Niels Bohr Institute, University of Copenhagen, 2100 Copenhagen, Denmark

(Dated: March 21, 2025)

We show that energy dissipation in slowly-driven, Markovian quantum systems at low temperature is linked to the geometry of the driving protocol through the quantum (or Fubini-Study) metric. Utilizing these findings, we establish lower bounds on dissipation rates in two-tone protocols, such as those employed for topological frequency conversion. Notably, in appropriate limits these bounds are only determined by the topology of the protocol and an effective quality factor of the system-bath coupling. Our results bridge topological and geometric phenomena with energy dissipation in open quantum systems, and further provide design principles for optimal driving protocols.

The geometry of quantum states [1, 2] is emerging as an important concept in condensed matter physics [3–26]. In particular, the *quantum* (or *Fubini-Study*) *metric* [27]—which defines a notion of distance on the manifold of quantum states—has been linked to various observable quantities including conductivity [14, 19], non-linear Hall effects [5, 6, 22, 23], optical responses [13, 16–18, 21] and superfluid stiffness [8–10, 20]. The renewed interest in the quantum metric provides a counterpoint to the much-studied effects of the Berry curvature in solids [1], as these two objects are obtained from the real and imaginary parts of a more general quantum geometric tensor.

Thermodynamics provides another context which hosts an emergent geometric description: namely, in quantum and classical systems a *dissipation metric* controls the energy dissipated by adiabatically traversing a path in parameter space [28–41]. This geometric picture then provides a simple operating principle to minimize dissipation or entropy production for a given task, by following geodesics on the corresponding manifold.

In this work we uncover a connection between these two distinct geometric notions. Considering slowly-driven quantum systems that are weakly coupled to a heat bath, we show that the low-temperature energy dissipation rate is controlled by geometric properties of the driving protocol through the quantum metric. We then exploit inequality relations between the quantum metric and Berry curvature [27, 42, 43] to establish various lower bounds on dissipation in a class of two-tone protocols [44] that support topological frequency conversion.

Setup.— We first focus on a two-level system subject to quasi-adiabatic driving, described by

$$H(t) = \mathbf{d}(t) \cdot \boldsymbol{\sigma}, \quad (1)$$

where $\boldsymbol{\sigma} = (\sigma_x, \sigma_y, \sigma_z)$ is a vector of Pauli matrices spanning the Hilbert space. The system is weakly coupled to a thermal bath at temperature T_B [45]. We consider the

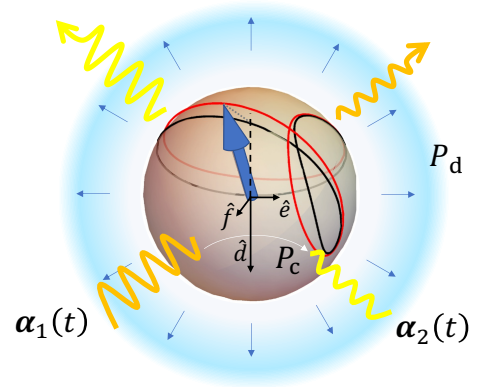


FIG. 1. The setup. A two-level system driven by the slowly-oscillating fields α_1 and α_2 and weakly coupled to a heat bath (represented by the blue halo). The black and red curves denote the trajectories of the Bloch-sphere vector $\mathbf{S}_0 = -\hat{\mathbf{d}}$ representing the instantaneous ground state, and the steady-state vector \mathbf{S}_{st} of the system, respectively. The instantaneous coordinate system consists of $\hat{\mathbf{d}}$, its normalized time derivative $\hat{\mathbf{e}} = \dot{\hat{\mathbf{d}}}/|\dot{\hat{\mathbf{d}}}|$ and $\hat{\mathbf{f}} = \hat{\mathbf{d}} \times \hat{\mathbf{e}}$. Leading diabatic corrections to the dynamics push the steady state in the $\hat{\mathbf{f}}$ direction, giving rise to energy pumping between α_1 and α_2 with rate P_c . The lag between \mathbf{S}_{st} and \mathbf{S}_0 induced by the heat bath (along the $\hat{\mathbf{e}}$ direction) leads to geometric energy dissipation with rate P_d .

Markovian limit [29, 46–54], where the coupling strength is weaker than the inverse correlation time of the bath, $1/\tau_c$, of order T_B for generic (e.g. Ohmic) baths. The dynamics of the density matrix $\rho(t)$ are then described by a master equation of the form

$$\dot{\rho}(t) = -i[H(t), \rho(t)] + \mathcal{D}(t)\{\rho(t)\}, \quad (2)$$

taking $\hbar = 1$ throughout. Here, the dissipator \mathcal{D} is a linear superoperator that depends on the details of the system, the thermal bath, and the system-bath coupling.

We consider cases where the time dependence of the Hamiltonian, $H(t)$, is slow compared to τ_c . In this regime, $\mathcal{D}(t)$ approaches the dissipator resulting from a static Hamiltonian—namely, one that relaxes the system towards instantaneous thermal equilibrium with the bath [50, 53, 54], captured by $\rho_{\text{eq}}(t) = e^{-\beta H(t)}/\text{Tr}[e^{-\beta H(t)}]$ with $\beta = 1/T_B$. However, the time dependence of Eq. (2) implies that its steady-state solution generally differs from $\rho_{\text{eq}}(t)$ due to diabatic corrections. As we describe in this work, such corrections cause geometric dissipation.

It is convenient to formally reexpress Eq. (2) as a Bloch equation [55] for the vector $\mathbf{S}(t) = \text{Tr}[\rho(t) \cdot \boldsymbol{\sigma}]$,

$$\dot{\mathbf{S}}(t) = 2\mathbf{d}(t) \times \mathbf{S}(t) - \Gamma(t)[\mathbf{S}(t) - \mathbf{S}_0(t)]. \quad (3)$$

Here the dissipator is reparametrized via the relaxation matrix $\Gamma_{ij}(t) = -\frac{1}{2}\text{Tr}[\sigma_i \mathcal{D}(t) \{\sigma_j\}]$, and $\mathbf{S}_0 = -\tanh(\beta\Delta/2)\hat{\mathbf{d}}$ denotes the Bloch vector corresponding to $\rho_{\text{eq}}(t)$ [56], with $\Delta = 2|\mathbf{d}|$ the spectral gap and $\hat{\mathbf{d}} \equiv \mathbf{d}/|\mathbf{d}|$. Focusing on the low-temperature limit where quantum geometric effects dominate, we set $\mathbf{S}_0 = -\hat{\mathbf{d}}$. Finite temperature corrections are discussed in the SM.

We consider dissipators that are isotropic with respect to $H(t)$. In this case, the most general form of the relaxation matrix [54] reads

$$\Gamma_{ij} = \frac{1}{\tau_1} \hat{\mathbf{d}}_i \hat{\mathbf{d}}_j + \frac{1}{\tau_2} (\delta_{ij} - \hat{\mathbf{d}}_i \hat{\mathbf{d}}_j) + \delta \epsilon_{ijk} \hat{\mathbf{d}}_k, \quad (4)$$

where τ_1, τ_2 are scalars that can be interpreted as longitudinal and transversal relaxation times in the instantaneous eigenbasis of the Hamiltonian, with $\tau_2 \leq 2\tau_1$ [57]. In the Supplementary Material (SM) [58] we derive Eqs. (2)-(4), with an explicit form of Γ , from a concrete microscopic model (see also Ref. [54]). The last term in Eq. (4) can be absorbed in Eq. (3) by rescaling the vector $\mathbf{d}(t)$ —we therefore set $\delta = 0$ for simplicity.

Low-temperature steady state and dissipation.—A steady-state solution to Eq. (3) can be found, up to leading order in diabatic corrections, by performing a rotating frame transformation [58],

$$\mathbf{S}_{\text{st}} = \frac{-(1 + \Delta^2 \tau_2^2) \hat{\mathbf{d}} + \tau_2 \dot{\hat{\mathbf{d}}} + \Delta \tau_2^2 (\hat{\mathbf{d}} \times \dot{\hat{\mathbf{d}}})}{1 + \Delta^2 \tau_2^2 + \tau_1 \tau_2 |\dot{\hat{\mathbf{d}}}|^2} + \mathcal{O}\left(\frac{|\dot{\hat{\mathbf{d}}}|^2}{\Delta^2}\right). \quad (5)$$

This result can be visualized with the help of Fig. 1. As the Hamiltonian varies in time, the direction of the Bloch vector $\hat{\mathbf{d}}$ changes. When driving is quasi-adiabatic, the steady state follows the trajectory of $-\hat{\mathbf{d}}(t)$ to remain close to the instantaneous ground state. Dissipation to the heat bath causes the spin to lag behind the Hamiltonian by the contribution $\propto \dot{\hat{\mathbf{d}}}$ in Eq. (5). There is also a diabatic correction to the coherent dynamics, due to the precession of the spin, that pushes the steady state

in the direction perpendicular to $\hat{\mathbf{d}}$ and $\dot{\hat{\mathbf{d}}}$, leading to the Berry curvature as discussed below.

In the steady state, the (long-time) average rate of energy dissipation, \bar{P}_d , equals the average rate of energy transfer into the system from the drive: $\bar{P}_d = \int_0^T \frac{dt}{T} \langle \dot{H}(t) \rangle$, where $\langle \dot{H}(t) \rangle = \dot{\mathbf{d}} \cdot \mathbf{S}_{\text{st}}$. Inserting \mathbf{S}_{st} from Eq. (5), to leading diabatic order we find

$$\bar{P}_d = \int_0^T \frac{dt}{T} \left[\frac{1}{2} \frac{\Delta \tau_2 |\dot{\hat{\mathbf{d}}}|^2 - \dot{\Delta} (1 + \Delta^2 \tau_2^2)}{1 + \Delta^2 \tau_2^2 + \tau_1 \tau_2 |\dot{\hat{\mathbf{d}}}|^2} \right]. \quad (6)$$

The dependence of \bar{P}_d on τ_2 may seem surprising, as dissipation in time-independent systems is set only by τ_1 . Its appearance is a consequence of the fact that τ_2 controls dephasing in the *instantaneous eigenbasis* of the Hamiltonian, while the steady-state Bloch vector \mathbf{S}_{st} lags behind $\mathbf{S}_0 = -\hat{\mathbf{d}}$, as shown in Eq. (5) and Fig. 1. Note that τ_1 still constrains dissipation: \bar{P}_d appropriately vanishes when $\tau_1 \rightarrow \infty$.

Focusing for the rest of this work on the typical case where $\tau_1 \sim \tau_2$ [59], Eq. (6) can be simplified by neglecting the higher-order diabatic contribution $\sim |\dot{\hat{\mathbf{d}}}|^2$ in the denominator. In this case the term proportional to $\dot{\Delta}$ vanishes when integrating over a period, as it can be rewritten as a total time derivative. We thus obtain

$$\bar{P}_d = \int_0^T \frac{dt}{T} \left[\frac{1}{4} \gamma |\dot{\hat{\mathbf{d}}}|^2 \right], \quad (7)$$

where $\gamma = \frac{2\Delta\tau_2}{1+\Delta^2\tau_2^2}$. In the limit of weak relaxation $\Delta\tau_2 \gg 1$, γ is proportional to the number of precession cycles within the relaxation time τ_2 , and can thus be understood as an effective inverse quality factor.

Geometric interpretation.— Let us assume that \mathbf{d} is controlled by a set of M parameters $(\alpha^1, \dots, \alpha^M) = \boldsymbol{\alpha}$ that are slowly changed over time: $\mathbf{d}(t) = \mathbf{d}(\boldsymbol{\alpha}(t))$. The average dissipation in Eq. (7) can then be written as an integral of a dissipation metric Λ over the path traced by time evolution,

$$\bar{P}_d = \int_0^T \frac{dt}{T} \Lambda_{ij} \dot{\alpha}^i \dot{\alpha}^j, \quad (8)$$

where

$$\Lambda_{ij} = \gamma G_{ij}, \quad G_{ij} = \frac{1}{4} \left(\partial_{\alpha^i} \hat{\mathbf{d}} \cdot \partial_{\alpha^j} \hat{\mathbf{d}} \right). \quad (9)$$

Here G is the quantum metric in the parameter space describing the driving fields, i and j label coordinates in M -dimensional space and Einstein summation convention is assumed throughout. This constitutes the main result of our work, and connects to earlier works on quantum thermodynamics [31, 32, 35–40] that provide an operating principle to minimize dissipation for a given task: the trajectory of $\boldsymbol{\alpha}(t)$ should follow a geodesic at uniform

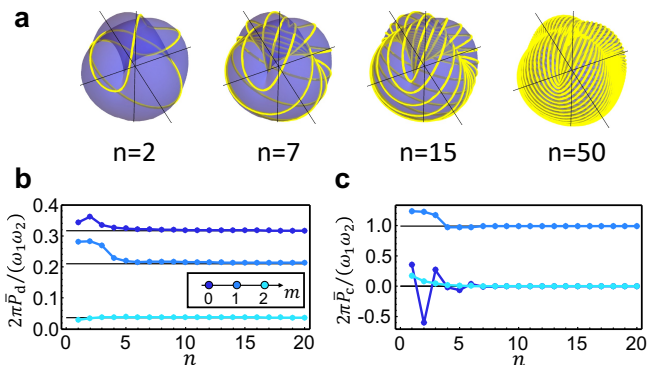


FIG. 2. **Approaching the incommensurate limit.** **a.** Trajectories on the surface $\mathbf{s} = \frac{1}{2}\sqrt{\gamma}\hat{\mathbf{d}}$, for different values of $\omega_2/\omega_1 = \frac{n}{n+1}$. **b.** Average dissipation rate along the “Lissajous curves” as a function of n . We use the driven spin model in Eq. (16) and consider $b_{11} = b_{22} = 1$, $b_{12} = b_{21} = 0.5$, $\theta = 0$, $\tau_2 = 10$, and three values of m indicated in the inset. **c.** Average frequency conversion rates as a function of n for the same parameters as in **b**, which quickly converge to the quantized result expected for incommensurate driving, Eq. (13).

speed on the surface defined by Λ . When γ is nearly constant this surface is described by $\mathbf{s} = \frac{1}{2}\sqrt{\gamma}\hat{\mathbf{d}}$, such that $\Lambda_{ij} = \partial_{\alpha^i}\mathbf{s} \cdot \partial_{\alpha^j}\mathbf{s}$, see Fig. 2a.

We can also generalize Eq. (9) for N -level systems [58]. Here the low-temperature dissipation metric $\Lambda^{(N)}$ instead involves a more complicated combination of quantum geometric and spectral quantities. Importantly, $\Lambda^{(N)}$ can be bounded from above and below in terms of the ground-state quantum metric, $G_{ij}^{(N)} = \frac{1}{2}\text{Tr}[\partial_{\alpha^i}P_0\partial_{\alpha^j}P_0]$, with $P_0(\boldsymbol{\alpha})$ the projector into the ground state of $H(\boldsymbol{\alpha})$:

$$G^{(N)} \succeq \Lambda^{(N)} \succeq \gamma^{(N)}G^{(N)}. \quad (10)$$

Here $A \succeq B$ implies that $A - B$ is positive semidefinite, and $\gamma^{(N)} = \min_n \frac{2\Delta_n\tau_{0n}}{1+\Delta_n^2\tau_{0n}^2}$, where Δ_n is the gap to the n -th excited state and τ_{0n} the relaxation time between the n -th excited state and the ground state.

Application to topological frequency conversion.—The connection between dissipation and quantum geometry uncovered above hints at a possible role of topology. To elucidate this role, we now specialize to time evolution characteristic of topological frequency conversion protocols [44], where $\boldsymbol{\alpha}(t) = \boldsymbol{\alpha}_1(t) + \boldsymbol{\alpha}_2(t)$ describes two harmonic drives with frequencies ω_1 and ω_2 , respectively (see Fig. 1). Here, the quantum metric in Eqs. (8), (9) can be re-expressed as a function of the two phases $\phi_a = \omega_a t$ (with $a = 1, 2$) describing the drives, reading $g_{ab} = G_{ij} \frac{\partial \alpha^i}{\partial \phi_a} \frac{\partial \alpha^j}{\partial \phi_b}$. The dissipation rate is then given by

$$\bar{P}_d = \omega_a \omega_b \int_0^T \frac{dt}{T} \gamma g_{ab}. \quad (11)$$

Similarly, the transferred power from mode 1 to mode 2 in the steady state can be calculated through $P_{12} =$

$\frac{1}{2} \left(\frac{\partial \mathbf{d}}{\partial \phi_1} \dot{\phi}_1 - \frac{\partial \mathbf{d}}{\partial \phi_2} \dot{\phi}_2 \right) \cdot \mathbf{S}_{\text{st}}$. This term is anti-symmetric in indices 1 and 2, and thus does not contribute to the net energy dissipation. Using the steady-state vector in Eq. (5), one obtains $P_{12} = \gamma \left[(\dot{\phi}_1)^2 g_{11} - (\dot{\phi}_2)^2 g_{22} \right] - P_c$. The first two terms denote the difference in energy dissipation due to each drive, and the frequency conversion power P_c averages to

$$\bar{P}_c = \omega_1 \omega_2 \int_0^T \frac{dt}{T} \left[\frac{\tau_2^2 \Delta^2}{1 + \tau_2^2 \Delta^2} \right] \Omega_{12}, \quad (12)$$

where $\Omega_{12} = \frac{1}{2} \hat{\mathbf{d}} \cdot \left(\partial_{\phi_1} \hat{\mathbf{d}} \times \partial_{\phi_2} \hat{\mathbf{d}} \right)$ is the Berry curvature associated with the phases of the two drives.

When the drive frequencies ω_1 and ω_2 are incommensurate, the system explores its entire phase space in the long-time limit. The averages in Eqs. (11) and (12) can then be replaced by an average over the phases $\phi_a = \omega_a t$, $\int_0^T \frac{dt}{T} \rightarrow \iint \frac{d\phi_1 d\phi_2}{4\pi^2}$. In the limit of weak relaxation $\Delta\tau_2 \gg 1$, the frequency conversion rate acquires a clear topological character, $\bar{P}_c = \frac{\omega_1 \omega_2}{2\pi} \mathcal{C}$, where

$$\mathcal{C} = \frac{1}{2\pi} \iint d\phi_1 d\phi_2 \Omega_{12} \quad (13)$$

is the corresponding Chern number, see Fig. 3a. In this regime, the two-level system transfers the energy of \mathcal{C} photons of mode 1 per period of mode 2 (or vice versa) between the two drives [44].

For commensurate frequencies ω_1 and ω_2 , the trajectory of $\boldsymbol{\alpha}(t)$ on the Bloch sphere is a “Lissajous” curve [60]. For a given ratio $\omega_2/\omega_1 = \frac{n}{n+1}$, with $n \in \mathbb{N}$, the time to complete one cycle increases as $T = (n+1)\frac{2\pi}{\omega_1}$, see Fig. 2a. We compute the dissipation and frequency conversion rates using Eqs. (11) and (12); the data are plotted in Figs. 2b,c. Both quantities rapidly converge for $n \gtrsim 5$ to their respective asymptotic values ($n \rightarrow \infty$) corresponding to incommensurate driving.

Bounds on dissipation and topology.—We now use the connection between energy dissipation and the quantum metric to derive lower bounds on dissipation for topological driving protocols. We consider a simple scenario in which the system and drives are in a symmetric configuration with $\bar{g}_{12} \equiv \iint d\phi_1 d\phi_2 g_{12} = 0$ (see SM [58] for an analysis of the general case where $\bar{g}_{12} \neq 0$.) In this case, the average dissipation in Eq. (11) arises only from the diagonal components of the quantum metric, proportional to $\omega_1^2 g_{11} + \omega_2^2 g_{22}$. These two terms can be bounded from below by $2\omega_1 \omega_2 \sqrt{g_{11} g_{22}} \geq 2\omega_1 \omega_2 \sqrt{\det g}$. Next, we use the identity $\sqrt{\det g} \geq |\Omega_{12}|/2$ (saturated for two-band models [42]), leading to a geometric lower bound on dissipation, $\bar{P}_d \geq \mathcal{B}_g$, where

$$\mathcal{B}_g = \omega_1 \omega_2 \iint \frac{d\phi_1 d\phi_2}{4\pi^2} \gamma |\Omega_{12}|. \quad (14)$$

The geometric bound is saturated when $\omega_1 \rightarrow \omega_2$ and the trace condition inequality [61] is saturated, $\text{Tr}[g] = |\Omega_{12}|$.

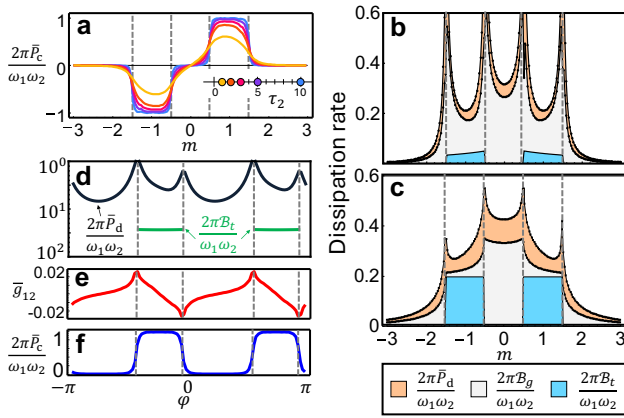


FIG. 3. Frequency conversion and bounds on dissipation. (a) Frequency conversion rate in the driven spin model, Eq. (16), as a function of m for $\theta = 0$ and different values of τ_2 indicated in the inset. In the limit $\tau_2 \rightarrow \infty$, $\bar{P}_c \rightarrow \frac{\omega_1 \omega_2}{2\pi} \mathcal{C}$, see Eq. (13). (b) Energy dissipation rate compared to the bounds in Eqs. (14) and (15), using the same parameters as in a and $\tau_2 = 10$. (c) *Idem* for the constant-gap Hamiltonian with $\Delta_0 = 1$. (d) Dissipation rate and the topological bound for $\theta = 0.2\pi$, $m = 1.2$, and $\tau_2 = 10$ as a function of φ . (e) The value of $\bar{g}_{12} = \iint g_{12} d\phi_1 d\phi_2$ and (f) the frequency conversion rate, for the same parameters as in d. We use $b_{11} = b_{22} = 1$ and $b_{12} = b_{21} = 0.5$ throughout.

A topological lower bound, $\mathcal{B}_t \leq \mathcal{B}_g$, can be obtained by replacing the term $\gamma(\phi_1, \phi_2)$ by its minimal value $\gamma_{\min} = \min_{\phi_1, \phi_2} \gamma(\phi_1, \phi_2)$, yielding

$$\mathcal{B}_t = \frac{\omega_1 \omega_2}{2\pi} \gamma_{\min} |\mathcal{C}|. \quad (15)$$

It follows from Eq. (15) that a finite frequency conversion rate ($|\mathcal{C}| > 0$) implies a minimum dissipation rate in the symmetric drive configuration. Further, \mathcal{B}_g in Eq. (14) provides a lower bound on dissipation for topologically-trivial protocols, with $\mathcal{C} = 0$, yet with a non-vanishing Berry curvature distribution.

Driven spin system.—To illustrate our results in a concrete physical setting, we consider a spin driven by two elliptically-polarized magnetic fields [44], $\mathbf{B}_1(t) = (0, b_{11} \sin \omega_1 t, b_{12} \cos \omega_1 t)$ and $\mathbf{B}_2(t) = (b_{21} \sin \omega_2 t, 0, b_{22} \cos \omega_2 t)$. The Hamiltonian reads

$$H(t) = \mathbf{m} \cdot \boldsymbol{\sigma} + (\mathbf{B}_1(t) + \mathbf{B}_2(t)) \cdot \boldsymbol{\sigma}, \quad (16)$$

where $\mathbf{m} = m(\sin \theta \cos \varphi, \sin \theta \sin \varphi, \cos \theta)$ is a time-independent Zeeman coupling. This model exhibits distinct topological regimes as a function of \mathbf{m} , characterized by $\mathcal{C} = \{-1, 0, 1\}$ (see Fig. 3a). For simplicity we take τ_2 to be time independent.

Figure 3b shows the dissipation in the different topological regimes of Eq. (16), calculated numerically using Eq. (11) for $\theta = 0$. For this value of θ , the symmetric drive condition is satisfied, $\bar{g}_{12} = \iint g_{12} d\phi_1 d\phi_2 = 0$; the energy dissipation rate is therefore bounded by \mathcal{B}_g and \mathcal{B}_t

[Eqs. (14) and (15)]. In the topological regimes ($\mathcal{C} \neq 0$), there is an obstruction to construct drives with arbitrarily low dissipation (for a fixed τ_2). The geometric bound \mathcal{B}_g tracks the actual dissipation even near the topological phase transition points (at $m = \pm 0.5, \pm 1.5$). Notice that the topological bound \mathcal{B}_t is not tight due to large variations of γ as a function of ϕ_1 and ϕ_2 . For Ohmic baths, which occur in many realistic settings, we expect γ to be approximately constant [50]. We therefore also consider a model with a constant value of γ by fixing $\Delta(t) = \Delta_0$, leading to a markedly improved bound \mathcal{B}_t compared to the time-dependent gap problem, see Fig. 3c.

Finally, we test the case $\bar{g}_{12} \neq 0$. To this end, we fix $\theta = 0.2\pi$, $m = 1.2$, and vary φ . The value and sign of \bar{g}_{12} evolve as a function of φ , see Fig. 3e, while the frequency conversion rate in Fig. 3f shows that the system correspondingly switches between different topological phases. Fig. 3d compares the dissipation to the topological bound \mathcal{B}_t in Eq. (15). While formally, \mathcal{B}_t is not valid when $\bar{g}_{12} < 0$, it provides a natural scale for the dissipation rate which is not reached in this model.

To estimate dissipation rates in this driven-spin example, let us consider an isolated cloud of N_c spin-1/2 atoms subjected to a time-dependent magnetic field [62–65]. Each atom weakly interacts with other identical atoms in its surroundings, acting as an effective heat bath. The energy dissipated by N_c atoms leads to an increase in the cloud’s temperature T_c , with the rate $\frac{dT_c}{dt} = N_c \bar{P}_d / C_c$, where C_c is the heat capacity of the cloud and \bar{P}_d the heating rate per spin. Assuming a magnetic field amplitude $|\mathbf{B}| \sim 2\pi \times 10$ KHz, frequencies $\omega_1, \omega_2 \sim 2\pi \times 1$ KHz, and relaxation time $\tau_2 \sim 1$ ms, we estimate $\gamma \approx 0.03$ and $\bar{P}_d \approx 2 \times 10^{-29}$ Watt, using Eq. (15). Finally, approximating $C_c \approx N_c k_B$, we find $\frac{dT_c}{dt} \approx 1.4 \mu\text{K/s}$. Given typical cloud temperatures on the order of $T_c \sim \text{nK}$, this heating rate should be experimentally accessible.

Summary and outlook.— In this work, we investigated energy dissipation from a slowly-driven quantum system to a cold heat bath, and showed that the dissipation rate is controlled by the quantum geometry of the driving protocol and the quality factor of the system-bath coupling [see Eqs. (8) and (9)]. The implications of our findings extend to a range of experimental platforms, such as nuclear spins [66], solids [60], superconducting qubits [67, 68], and cavity QED [69].

Remarkably, in a class of driving protocols (such as those hosting topological frequency conversion), the system inevitably generates heat at a rate no lower than that given by Eqs. (14) and (15), for a symmetric configuration of the drives. Interestingly, for an asymmetric drive configuration, the theoretical minimal dissipation rate can (in principle) be reduced due to interference between the two drives. However, we were not able to identify configurations that violate the topological bound; this may however provide a promising direction for designing low-dissipation driving protocols.

In this study, we focused on a specific class of isotropic dissipators valid to leading order in diabatic corrections. In general, heat baths derived from microscopic models [50, 52, 53] may contain non-isotropic as well as sub-leading diabatic corrections that may lead to relevant contributions to dissipation; their examination is left for future work. Another intriguing direction for further study concerns dissipation in multi-qubit adiabatic computational protocols [70, 71], where heating can result in an increased error rate [72] and loss of quantum information. Systems with spatial structure (such as quantum pumps [73]) also constitute an intriguing platform where driving can induce heat currents. Finally, it would be interesting to explore extensions of our results beyond the average properties of dissipation, considering *e.g.* the statistics (or higher moments) of dissipated heat [74, 75].

Acknowledgments.— We thank Jason Alicea, Israel Klich, Nandagopal Manoj, Johannes Mitscherling, Valerio Peri, and Mark Rudner for insightful discussions. É. L.-H. was supported by the Gordon and Betty Moore Foundation’s EPiQS Initiative, Grant GBMF8682. F.N. was supported by the U.S. Department of Energy, Office of Science, Basic Energy Sciences under award DE-SC0019166, the Simons Foundation under award 623768, and the Carlsberg Foundation, grant CF22-0727. G.R. and I.E. are grateful for support from the Simons Foundation and the Institute of Quantum Information and Matter. G.R. is grateful for support from the ARO MURI grant FA9550-22-1-0339. This work was performed in part at Aspen Center for Physics, which is supported by National Science Foundation grant PHY-221045.

-
- [1] D. Xiao, M.-C. Chang, and Q. Niu, Berry phase effects on electronic properties, *Rev. Mod. Phys.* **82**, 1959 (2010).
- [2] R. Resta, The insulating state of matter: a geometrical theory, *Eur. Phys. J. B* **79**, 121–137 (2011).
- [3] T. Neupert, C. Chamon, and C. Mudry, Measuring the quantum geometry of Bloch bands with current noise, *Phys. Rev. B* **87**, 245103 (2013).
- [4] M. Kolodrubetz, V. Gritsev, and A. Polkovnikov, Classifying and measuring geometry of a quantum ground state manifold, *Phys. Rev. B* **88**, 064304 (2013).
- [5] Y. Gao, S. A. Yang, and Q. Niu, Field induced positional shift of Bloch electrons and its dynamical implications, *Phys. Rev. Lett.* **112**, 166601 (2014).
- [6] I. Sodemann and L. Fu, Quantum nonlinear Hall effect induced by Berry curvature dipole in time-reversal invariant materials, *Phys. Rev. Lett.* **115**, 216806 (2015).
- [7] Y. Gao, S. A. Yang, and Q. Niu, Geometrical effects in orbital magnetic susceptibility, *Phys. Rev. B* **91**, 214405 (2015).
- [8] S. Peotta and P. Törmä, Superfluidity in topologically nontrivial flat bands, *Nat. Commun.* **6** (2015).
- [9] A. Julku, S. Peotta, T. I. Vanhala, D.-H. Kim, and P. Törmä, Geometric origin of superfluidity in the Lieb-lattice flat band, *Phys. Rev. Lett.* **117**, 045303 (2016).
- [10] L. Liang, T. I. Vanhala, S. Peotta, T. Siro, A. Harju, and P. Törmä, Band geometry, Berry curvature, and superfluid weight, *Phys. Rev. B* **95**, 024515 (2017).
- [11] O. Bleu, G. Malpuech, Y. Gao, and D. D. Solnyshkov, Effective theory of nonadiabatic quantum evolution based on the quantum geometric tensor, *Phys. Rev. Lett.* **121**, 020401 (2018).
- [12] Y. Gao and D. Xiao, Nonreciprocal directional dichroism induced by the quantum metric dipole, *Phys. Rev. Lett.* **122**, 227402 (2019).
- [13] T. Holder, D. Kaplan, and B. Yan, Consequences of time-reversal-symmetry breaking in the light-matter interaction: Berry curvature, quantum metric, and diabatic motion, *Phys. Rev. Res.* **2**, 033100 (2020).
- [14] J. Mitscherling, Longitudinal and anomalous Hall conductivity of a general two-band model, *Phys. Rev. B* **102**, 165151 (2020).
- [15] E. Rossi, Quantum metric and correlated states in two-dimensional systems, *Curr. Opin. Solid State Mater. Sci.* **25**, 100952 (2021).
- [16] J. Ahn, G.-Y. Guo, N. Nagaosa, and A. Vishwanath, Riemannian geometry of resonant optical responses, *Nat. Phys.* **18**, 290–295 (2021).
- [17] S. Takayoshi, J. Wu, and T. Oka, Nonadiabatic nonlinear optics and quantum geometry — application to the twisted Schwinger effect, *SciPost Phys.* **11**, 075 (2021).
- [18] P. Bhalla, K. Das, D. Culcer, and A. Agarwal, Resonant second-harmonic generation as a probe of quantum geometry, *Phys. Rev. Lett.* **129**, 227401 (2022).
- [19] J. Mitscherling and T. Holder, Bound on resistivity in flat-band materials due to the quantum metric, *Phys. Rev. B* **105**, 085154 (2022).
- [20] P. Törmä, S. Peotta, and B. A. Bernevig, Superconductivity, superfluidity and quantum geometry in twisted multilayer systems, *Nat. Rev. Phys.* **4**, 528 (2022).
- [21] M. Lysne, M. Schüler, and P. Werner, Quantum optics measurement scheme for quantum geometry and topological invariants, *Phys. Rev. Lett.* **131**, 156901 (2023).
- [22] N. Wang, D. Kaplan, Z. Zhang, T. Holder, N. Cao, A. Wang, X. Zhou, F. Zhou, Z. Jiang, C. Zhang, S. Ru, H. Cai, K. Watanabe, T. Taniguchi, B. Yan, and W. Gao, Quantum-metric-induced nonlinear transport in a topological antiferromagnet, *Nature* **621**, 487–492 (2023).
- [23] A. Gao, Y.-F. Liu, J.-X. Qiu, B. Ghosh, T. V. Trevisan, Y. Onishi, C. Hu, T. Qian, H.-J. Tien, S.-W. Chen, M. Huang, D. Bérubé, H. Li, C. Tzschaschel, T. Dinh, Z. Sun, S.-C. Ho, S.-W. Lien, B. Singh, K. Watanabe, T. Taniguchi, D. C. Bell, H. Lin, T.-R. Chang, C. R. Du, A. Bansil, L. Fu, N. Ni, P. P. Orth, Q. Ma, and S.-Y. Xu, Quantum metric nonlinear Hall effect in a topological antiferromagnetic heterostructure, *Science* **381**, 181–186 (2023).
- [24] D. Kaplan, T. Holder, and B. Yan, Unification of nonlinear anomalous Hall effect and nonreciprocal magnetoresistance in metals by the quantum geometry, *Phys. Rev. Lett.* **132**, 026301 (2024).
- [25] I. Komissarov, T. Holder, and R. Queiroz, The quantum geometric origin of capacitance in insulators, *Nat. Commun.* **15** (2024).
- [26] W. J. Jankowski, A. S. Morris, A. Bouhon, F. N. Ünal, and R.-J. Slager, Optical manifestations and bounds of topological Euler class, *Phys. Rev. B* **111**, L081103 (2025).

- [27] J. P. Provost and G. Vallee, Riemannian structure on manifolds of quantum states, *Commun. Math. Phys.* **76**, 289 (1980).
- [28] J. E. Avron, M. Fraas, G. M. Graf, and P. Grech, Optimal time schedule for adiabatic evolution, *Phys. Rev. A* **82**, 040304(R) (2010).
- [29] J. E. Avron, M. Fraas, G. M. Graf, and O. Kenneth, Quantum response of dephasing open systems, *New J. Phys.* **13**, 053042 (2011).
- [30] J. E. Avron, M. Fraas, and G. M. Graf, Adiabatic response for lindblad dynamics, *J. Stat. Phys.* **148**, 800 (2012).
- [31] D. A. Sivak and G. E. Crooks, Thermodynamic metrics and optimal paths, *Phys. Rev. Lett.* **108**, 190602 (2012).
- [32] P. R. Zulkowski and M. R. DeWeese, Optimal protocols for slowly driven quantum systems, *Phys. Rev. E* **92**, 032113 (2015).
- [33] M. F. Ludovico, F. Battista, F. von Oppen, and L. Arrachea, Adiabatic response and quantum thermoelectrics for ac-driven quantum systems, *Phys. Rev. B* **93**, 075136 (2016).
- [34] M. Bukov, D. Sels, and A. Polkovnikov, Geometric speed limit of accessible many-body state preparation, *Phys. Rev. X* **9**, 011034 (2019).
- [35] M. Scandi and M. Perarnau-Llobet, Thermodynamic length in open quantum systems, *Quantum* **3**, 197 (2019).
- [36] P. Abiuso, H. J. D. Miller, M. Perarnau-Llobet, and M. Scandi, Geometric optimisation of quantum thermodynamic processes, *Entropy* **22**, 1076 (2020).
- [37] B. Bhandari, P. T. Alonso, F. Taddei, F. von Oppen, R. Fazio, and L. Arrachea, Geometric properties of adiabatic quantum thermal machines, *Phys. Rev. B* **102**, 155407 (2020).
- [38] D. Loutchko, Y. Sughiyama, and T. J. Kobayashi, Riemannian geometry of optimal driving and thermodynamic length and its application to chemical reaction networks, *Phys. Rev. Research* **4**, 043049 (2022).
- [39] P. Terrén Alonso, P. Abiuso, M. Perarnau-Llobet, and L. Arrachea, Geometric optimization of nonequilibrium adiabatic thermal machines and implementation in a qubit system, *PRX Quantum* **3**, 010326 (2022).
- [40] L. Arrachea, Energy dynamics, heat production and heat-work conversion with qubits: toward the development of quantum machines, *Reports on Progress in Physics* **86**, 036501 (2023).
- [41] T. Morimoto, S. Kitamura, and N. Nagaosa, Geometric aspects of nonlinear and nonequilibrium phenomena, *J. Phys. Soc. Jpn.* **92**, 072001 (2023).
- [42] T. Ozawa and B. Mera, Relations between topology and the quantum metric for chern insulators, *Phys. Rev. B* **104**, 045103 (2021).
- [43] A. Graf and F. Piéchon, Berry curvature and quantum metric in n -band systems: An eigenprojector approach, *Phys. Rev. B* **104**, 085114 (2021).
- [44] I. Martin, G. Refael, and B. Halperin, Topological frequency conversion in strongly driven quantum systems, *Phys. Rev. X* **7**, 041008 (2017).
- [45] A. J. Leggett, S. Chakravarty, A. T. Dorsey, M. P. A. Fisher, A. Garg, and W. Zwerger, Dynamics of the dissipative two-state system, *Rev. Mod. Phys.* **59**, 1 (1987).
- [46] R. Alicki, The quantum open system as a model of the heat engine, *J. Phys. A* **12**, L103 (1979).
- [47] R. Blümel, A. Buchleitner, R. Graham, L. Sirko, U. Smilansky, and H. Walther, Dynamical localization in the microwave interaction of rydberg atoms: The influence of noise, *Phys. Rev. A* **44**, 4521 (1991).
- [48] S. Kohler, T. Dittrich, and P. Hänggi, Floquet-markovian description of the parametrically driven, dissipative harmonic quantum oscillator, *Phys. Rev. E* **55**, 300 (1997).
- [49] H.-P. Breuer, W. Huber, and F. Petruccione, Quasistationary distributions of dissipative nonlinear quantum oscillators in strong periodic driving fields, *Phys. Rev. E* **61**, 4883 (2000).
- [50] H.-P. Breuer, F. Petruccione, H.-P. Breuer, and F. Petruccione, *The Theory of Open Quantum Systems* (Oxford University Press, Oxford, New York, 2007).
- [51] D. W. Hone, R. Ketzmerick, and W. Kohn, Statistical mechanics of floquet systems: The pervasive problem of near degeneracies, *Phys. Rev. E* **79**, 051129 (2009).
- [52] E. Mozgunov and D. Lidar, Completely positive master equation for arbitrary driving and small level spacing, *Quantum* **4**, 227 (2020).
- [53] F. Nathan and M. S. Rudner, Universal lindblad equation for open quantum systems, *Phys. Rev. B* **102**, 115109 (2020).
- [54] G. D. Meglio, M. B. Plenio, and S. F. Huelga, *Time dependent markovian master equation beyond the adiabatic limit* (2023), arXiv:2304.06166 [quant-ph].
- [55] F. Bloch, Nuclear induction, *Phys. Rev.* **70**, 460 (1946).
- [56] For a general dissipator $\mathcal{D}(t)$, $\mathbf{S}_0(t)$ can be defined from \mathcal{D} as $\mathbf{S}_0 = \frac{\Gamma^{-1}(t)}{2} \text{Tr}[\sigma \mathcal{D}(t)\{1\}]$.
- [57] M. H. Levitt, *Spin dynamics: Basics of Nuclear Magnetic Resonance*, 2nd ed. (Wiley-Blackwell, Hoboken, NJ, 2008).
- [58] See Supplemental Material for details.
- [59] This condition can be extended to $\tau_2/\tau_1 \gg |\dot{\mathbf{d}}|^2/\Delta^2$.
- [60] F. Nathan, I. Martin, and G. Refael, Topological frequency conversion in weyl semimetals, *Phys. Rev. Research* **4**, 043060 (2022).
- [61] R. Roy, Band geometry of fractional topological insulators, *Phys. Rev. B* **90**, 165139 (2014).
- [62] J. Zhang, G. Pagano, P. W. Hess, A. Kyprianidis, P. Becker, H. Kaplan, A. V. Gorshkov, Z.-X. Gong, and C. Monroe, Observation of a many-body dynamical phase transition with a 53-qubit quantum simulator, *Nature* **551**, 601 (2017).
- [63] C. Monroe, W. C. Campbell, L.-M. Duan, Z.-X. Gong, A. V. Gorshkov, P. W. Hess, R. Islam, K. Kim, N. M. Linke, G. Pagano, P. Richerme, C. Senko, and N. Y. Yao, Programmable quantum simulations of spin systems with trapped ions, *Rev. Mod. Phys.* **93**, 025001 (2021).
- [64] A. Periwal, E. S. Cooper, P. Kunkel, J. F. Wienand, E. J. Davis, and M. Schleier-Smith, Programmable interactions and emergent geometry in an array of atom clouds, *Nature* **600**, 630–635 (2021).
- [65] L. Feng, O. Katz, C. Haack, M. Maghrebi, A. V. Gorshkov, Z. Gong, M. Cetina, and C. Monroe, Continuous symmetry breaking in a trapped-ion spin chain, *Nature* **623**, 713–717 (2023).
- [66] J. A. Jones, V. Vedral, A. Ekert, and G. Castagnoli, Geometric quantum computation using nuclear magnetic resonance, *Nature* **403**, 869 (2000).
- [67] D. Malz and A. Smith, Topological two-dimensional floquet lattice on a single superconducting qubit, *Phys. Rev. Lett.* **126**, 163602 (2021).
- [68] E. Gümüş, D. Majidi, D. Nikolić, P. Raif, B. Karimi, J. T. Peltonen, E. Scheer, J. P. Pekola, H. Courtois, W. Belzig, and C. B. Winkelmann, Calorimetry of a phase slip in a

- josephson junction, *Nat. Phys.* **19**, 196 (2023).
- [69] D. M. Long, P. J. D. Crowley, A. J. Kollár, and A. Chandran, Boosting the quantum state of a cavity with floquet driving, *Phys. Rev. Lett.* **128**, 183602 (2022).
- [70] M. S. Sarandy and D. A. Lidar, Adiabatic quantum computation in open systems, *Phys. Rev. Lett.* **95**, 250503 (2005).
- [71] T. Albash and D. A. Lidar, Adiabatic quantum computation, *Rev. Mod. Phys.* **90**, 015002 (2018).
- [72] T. Albash and D. A. Lidar, Decoherence in adiabatic quantum computation, *Phys. Rev. A* **91**, 062320 (2015).
- [73] R. Citro and M. Aidelsburger, Thouless pumping and topology, *Nat. Rev. Phys.* **5**, 87 (2023).
- [74] C. Jarzynski and D. K. Wójcik, Classical and quantum fluctuation theorems for heat exchange, *Phys. Rev. Lett.* **92**, 230602 (2004).
- [75] K. Funo and H. T. Quan, Path integral approach to heat in quantum thermodynamics, *Phys. Rev. E* **98**, 012113 (2018).

Quantum geometry and bounds on dissipation in slowly driven quantum systems - Supplementary material

Iliya Esin,^{1,2} Étienne Lantagne-Hurtubise,^{1,3} Frederik Nathan,^{1,4} and Gil Refael¹

¹*Department of Physics and Institute for Quantum Information and Matter,
California Institute of Technology, Pasadena, California 91125, USA*

²*Department of Physics, Bar-Ilan University, 52900, Ramat Gan, Israel*

³*Département de Physique and Institut Quantique,*

Université de Sherbrooke, Sherbrooke, Québec, Canada J1K 2R1

⁴*Center for Quantum Devices and NNF Quantum Computing Programme,
Niels Bohr Institute, University of Copenhagen, 2100 Copenhagen, Denmark*

(Dated: March 21, 2025)

Here, we present expanded derivations of the key results in the main text and additional discussions. We assume throughout $\hbar = 1$.

HIERARCHY OF ENERGY SCALES

To organize our expansion we consider the following hierarchy of energy scales, summarized in Fig. S1. We assume that the gap Δ is the largest energy scale in the problem, with the driving frequency ω , the system-bath coupling strength $\lambda \sim \|\Gamma\|$, and the inverse correlation time of the bath τ_c^{-1} (commonly determined by the bath temperature T_B [1]) all much smaller than Δ . In particular, this hierarchy includes the assumption of adiabaticity, $\omega \ll \Delta$.

In order to neglect non-Markovian corrections arising from the coupling to the bath we further assume that $\lambda \ll \tau_c^{-1} \sim T_B$. The assumption of instantaneous thermal equilibrium, whereby the dissipator (at any given time t) tends to relax the system towards its instantaneous thermal equilibrium state with the bath, is justified in the limit $\omega \ll \tau_c^{-1}$. However, the relationship between ω and λ can remain general, ranging from the under-damped ($\lambda \ll \omega$) through the over-damped ($\omega \ll \lambda$) regime.

STEADY STATE SOLUTION OF THE BLOCH EQUATION

Here we find the steady state solution to the Bloch equation [Eq. (3) in the main text],

$$\dot{\mathbf{S}}(t) = 2\mathbf{d}(t) \times \mathbf{S}(t) - \Gamma(t)(\mathbf{S}(t) - \mathbf{S}_0(t)), \quad (\text{S1})$$

and compute the steady-state dissipation rate. In the following we will use the relaxation-time approximation dissipator that takes the form

$$\Gamma_{ij}(t) = \frac{1}{\tau_1(t)} \hat{\mathbf{d}}_i(t) \hat{\mathbf{d}}_j(t) + \frac{1}{\tau_2(t)} (\delta_{ij} - \hat{\mathbf{d}}_i(t) \hat{\mathbf{d}}_j(t)). \quad (\text{S2})$$

This expression describes the most general isotropic dissipator, i.e., symmetric under rotations around the axis of the instantaneous Hamiltonian represented by $\hat{\mathbf{d}}(t)$ – see Eq. (4) in the main text, where the term proportional to

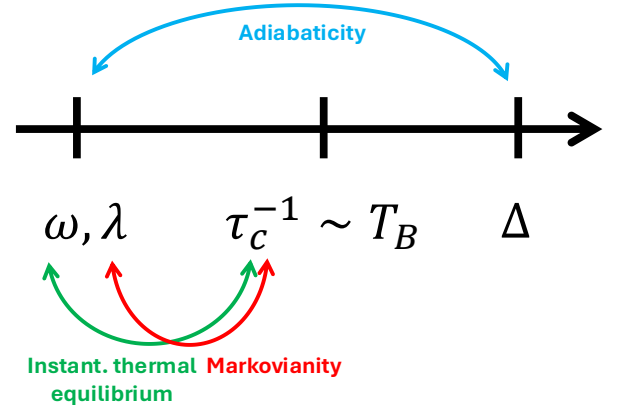


FIG. S1. Hierarchy of energy scales assumed in our work. Here ω denotes the driving frequency, $\lambda \sim \|\Gamma\|$ the characteristic system-bath coupling strength, τ_c the intrinsic correlation time of the bath, T_B the bath temperature and Δ the energy gap in the system. Various physical conditions imposed on our steady-state solution are highlighted by colored arrows.

δ can be absorbed in a redefinition of the instantaneous gap.

We now perform a time-dependent rotation $R(t)$ that maps Eq. (S1) into an equation of the same form, but in a different frame, where $\hat{\mathbf{d}}(t)$ points in the $\hat{\mathbf{z}}$ direction:

$$R\hat{\mathbf{d}} = \hat{\mathbf{z}}. \quad (\text{S3})$$

The spin in the transformed frame, $\mathbf{S}' = R\mathbf{S}$, evolves according to the differential equation

$$\dot{\mathbf{S}}' = \Delta\hat{\mathbf{z}} \times \mathbf{S}' + \dot{R}R^{-1}\mathbf{S}' - \Gamma'(\mathbf{S}' - \mathbf{S}'_0) \quad (\text{S4})$$

with $\Gamma' = R\Gamma R^{-1}$, and $\mathbf{S}'_0 = R\mathbf{S}_0$. At low temperature the system's ground state is parametrized by $\mathbf{S}_0 = -\hat{\mathbf{d}}$, hence we have $\mathbf{S}'_0 = -\hat{\mathbf{z}}$. The advantage of this frame transformation is that the time dependence of $\mathbf{d}(t)$ has been partially accounted for: \mathbf{d} now points along the $\hat{\mathbf{z}}$ axis and its time dependence only comes through its

magnitude $\Delta(t)$. Such a time-dependent frame transformation, however, comes with the Berry connection term $\dot{R}R^{-1}$ which can be simplified in the following way. First, note that $\dot{R}R^{-1}$ is a generator of rotations, and thus is a real and anti-symmetric three dimensional matrix – this can be seen from

$$\left(\dot{R}R^{-1}\right)^T = R\dot{R}^{-1} = -\dot{R}R^{-1}, \quad (\text{S5})$$

where we used $R^{-1} = R^T$ for rotation matrices and $\partial_t(RR^{-1}) = 0$. Therefore, the action of such a matrix on the spin vector \mathbf{S}' can be equivalently represented as a cross product with some real vector \mathbf{g}' , $\dot{R}R^{-1}\mathbf{S}' = \mathbf{g}' \times \mathbf{S}'$. In order to find \mathbf{g}' , we notice that because the new frame of reference has a time-independent axis, we can write

$$\partial_t(\hat{\mathbf{z}} = R\hat{\mathbf{d}}) = \dot{R}\hat{\mathbf{d}} + R\dot{\hat{\mathbf{d}}} = 0. \quad (\text{S6})$$

This condition is fulfilled if R is given by the solution to the differential equation

$$\dot{R}\mathbf{v} = -R\left[(\hat{\mathbf{d}} \times \dot{\hat{\mathbf{d}}}) \times \mathbf{v}\right] \quad (\text{S7})$$

for any vector \mathbf{v} , with initial condition $R(0) = R_0$ where R_0 is some orthogonal matrix satisfying $R_0\hat{\mathbf{d}}(0) = \hat{\mathbf{z}}$; note that this differential equation satisfies $\dot{R}\mathbf{v} \perp R\mathbf{v}$, implying that the solution is an orthogonal matrix, as we require. To see why this choice of R satisfies Eq. (S6), note that setting $\mathbf{v} = \hat{\mathbf{d}}$ results in $\dot{R}\hat{\mathbf{d}} = -R\dot{\hat{\mathbf{d}}}$.

Using Eq. (S7), we arrive at

$$\dot{R}(R^{-1}\mathbf{S}') = -R\left[(\hat{\mathbf{d}} \times \dot{\hat{\mathbf{d}}}) \times R^{-1}\mathbf{S}'\right] = -\left[R(\hat{\mathbf{d}} \times \dot{\hat{\mathbf{d}}})\right] \times \mathbf{S}'. \quad (\text{S8})$$

We therefore identify $\mathbf{g}' = -R(\hat{\mathbf{d}} \times \dot{\hat{\mathbf{d}}})$ and write Eq. (S1) in the transformed coordinate system as

$$\dot{\mathbf{S}}' = \left[\Delta\hat{\mathbf{z}} - R(\hat{\mathbf{d}} \times \dot{\hat{\mathbf{d}}})\right] \times \mathbf{S}' - \Gamma'(\mathbf{S}' + \hat{\mathbf{z}}). \quad (\text{S9})$$

where we used $\mathbf{S}'_0 = -\hat{\mathbf{z}}$ at zero temperature.

Exactly solvable toy model

To gain intuition, we first consider a solvable toy model, where the Hamiltonian rotates periodically in time along a circular trajectory with $\mathbf{d} = \frac{1}{2}\Delta_0(\sin\omega t, \cos\omega t, 0)$, with a constant gap $\Delta = \Delta_0$. The time-dependent frame rotation R rotates $\hat{\mathbf{d}}$ to the $\hat{\mathbf{z}}$ axis; we take the explicit form $R = R_x(\pi/2)R_z(\omega t)$, such that $R(\hat{\mathbf{d}} \times \dot{\hat{\mathbf{d}}}) = \omega\hat{\mathbf{y}}$. The orthonormal rotating-frame basis $(\hat{\mathbf{x}}, \hat{\mathbf{y}}, \hat{\mathbf{z}})$ is completed by identifying $R(\dot{\hat{\mathbf{d}}}) = \omega\hat{\mathbf{x}}$, thus preserving the right-hand rule. The Bloch equation in the rotating frame then takes the form

$$\dot{\mathbf{S}}' = [\Delta_0\hat{\mathbf{z}} - \omega\hat{\mathbf{y}}] \times \mathbf{S}' - \Gamma'(\mathbf{S}' + \hat{\mathbf{z}}), \quad (\text{S10})$$

which is now time independent. The dissipator in the rotating frame is taken to follow the relaxation-time approximation, Eq. (S2), with $\Gamma' = R\Gamma R^T = \text{diag}(1/\tau_2, 1/\tau_2, 1/\tau_1)$. The steady-state solution is obtained by setting the left-hand side of Eq. (S10) to 0, leading to

$$\mathbf{S}'_{\text{st}} = -\frac{1}{\tau_1}(M)^{-1}\hat{\mathbf{z}}, \quad (\text{S11})$$

where M is the matrix defined by $M\mathbf{v} = [\omega\hat{\mathbf{y}} - \Delta_0\hat{\mathbf{z}}] \times \mathbf{v} + \Gamma'\mathbf{v}$. In the example we consider,

$$M = \begin{pmatrix} 1/\tau_2 & \Delta_0 & \omega \\ -\Delta_0 & 1/\tau_2 & 0 \\ -\omega & 0 & 1/\tau_1 \end{pmatrix} \quad (\text{S12})$$

in the orthonormal basis defined by $(\hat{\mathbf{x}}, \hat{\mathbf{y}}, \hat{\mathbf{z}})$. Inverting M and substituting in Eq. (S11), we find the steady-state solution

$$\mathbf{S}'_{\text{st}} = \frac{1}{1 + \Delta_0^2\tau_2^2 + \tau_1\tau_2\omega^2} \begin{pmatrix} \tau_2\omega \\ \Delta_0\omega\tau_2^2 \\ -1 - \Delta_0^2\tau_2^2 \end{pmatrix}. \quad (\text{S13})$$

The dissipated power is obtained through $P_d = \dot{\mathbf{d}} \cdot \mathbf{S}_{\text{st}} = \frac{1}{2}\Delta_0\dot{\hat{\mathbf{d}}} \cdot \mathbf{S}_{\text{st}} = \frac{1}{2}\Delta_0\omega\hat{\mathbf{x}} \cdot \mathbf{S}'_{\text{st}}$, as the transformation between frames maps $(\hat{\mathbf{x}}, \hat{\mathbf{y}}, \hat{\mathbf{z}}) \leftrightarrow (\frac{\dot{\hat{\mathbf{d}}}}{\omega}, \frac{\hat{\mathbf{d}} \times \dot{\hat{\mathbf{d}}}}{\omega}, \hat{\mathbf{d}})$. Thus,

$$P_d = \frac{1}{2} \frac{\Delta_0\tau_2\omega^2}{1 + \Delta_0^2\tau_2^2 + \tau_1\tau_2\omega^2}. \quad (\text{S14})$$

Back to the general case

With the intuition from the above toy model in mind, we now come back to the case where the system is driven by an arbitrary (but slow) drive. The problem posed by Eq. (S9) is now time dependent, but the time dependence is of order ω/Δ , where $\omega \sim |\dot{\hat{\mathbf{d}}}|$. More precisely, as we will see we can once again set the left-hand-side of Eq. (S9) to zero, because $\dot{\mathbf{S}}'$ only contains terms at order $\mathcal{O}(\omega^2/\Delta^2)$ or higher.

We can then solve for the (now time-dependent) steady state in the rotating frame in a similar way. To parametrize a more general time evolution we consider

$$R(\hat{\mathbf{d}} \times \dot{\hat{\mathbf{d}}}) = |\dot{\hat{\mathbf{d}}}|R(\hat{\mathbf{f}}) = |\dot{\hat{\mathbf{d}}}|(a\hat{\mathbf{x}} + b\hat{\mathbf{y}}), \quad (\text{S15})$$

with a and b time-dependent functions parametrizing rotations, normalized such that at all times $a^2 + b^2 = 1$, and we defined the unit vector $\hat{\mathbf{f}} \equiv (\hat{\mathbf{d}} \times \dot{\hat{\mathbf{d}}})/|\hat{\mathbf{d}} \times \dot{\hat{\mathbf{d}}}| =$

$(\hat{\mathbf{d}} \times \dot{\hat{\mathbf{d}}})/|\dot{\hat{\mathbf{d}}}|$. (Note that a component proportional to $\hat{\mathbf{z}}$ is not allowed in Eq. (S15) because $\hat{\mathbf{d}} \times \dot{\hat{\mathbf{d}}}$ must always be perpendicular to $\hat{\mathbf{d}}$.) To complete the basis transformation, we define the unit vector $\hat{\mathbf{e}} = \dot{\hat{\mathbf{d}}}/|\dot{\hat{\mathbf{d}}}|$ such that $\hat{\mathbf{f}} = \hat{\mathbf{d}} \times \hat{\mathbf{e}}$. In the rotating frame basis this unit vector is mapped to

$$R(\hat{\mathbf{e}}) = (b\hat{\mathbf{x}} - a\hat{\mathbf{y}}). \quad (\text{S16})$$

The instantaneous steady-state equation in the rotating $(\hat{\mathbf{x}}, \hat{\mathbf{y}}, \hat{\mathbf{z}})$ basis follows the form of Eq. (S11), but with a time-dependent matrix

$$M = \begin{pmatrix} 1/\tau_2 & \Delta & b|\dot{\hat{\mathbf{d}}}| \\ -\Delta & 1/\tau_2 & -a|\dot{\hat{\mathbf{d}}}| \\ -b|\dot{\hat{\mathbf{d}}}| & a|\dot{\hat{\mathbf{d}}}| & 1/\tau_1 \end{pmatrix}. \quad (\text{S17})$$

Its expression is simpler when transforming back to the original (laboratory) frame with basis vectors $(\hat{\mathbf{e}}, \hat{\mathbf{f}}, \hat{\mathbf{d}})$:

$$\mathbf{S}_{\text{st}} = \frac{1}{1 + \Delta^2\tau_2^2 + \tau_1\tau_2|\dot{\hat{\mathbf{d}}}|^2} \begin{pmatrix} |\dot{\hat{\mathbf{d}}}| \tau_2 \\ |\dot{\hat{\mathbf{d}}}| \Delta \tau_2^2 \\ -1 - \Delta^2\tau_2^2 \end{pmatrix}, \quad (\text{S18})$$

as reported in the main text, see Eq. (5). This steady-state solution admits a time derivative that is at least of order ω^2/Δ^2 , thus justifying our setting the left-hand side of Eq. (S9) to zero to order ω/Δ .

We then compute dissipation, using the laboratory-frame steady state obtained in Eq. (S18):

$$\begin{aligned} P_d &= \dot{\mathbf{d}} \cdot \mathbf{S}_{\text{st}} = \frac{1}{2} \Delta \dot{\hat{\mathbf{d}}} \cdot \mathbf{S}_{\text{st}} + \frac{1}{2} \dot{\Delta} \hat{\mathbf{d}} \cdot \mathbf{S}_{\text{st}} \\ &= \frac{1}{2} \frac{\Delta \tau_2 |\dot{\hat{\mathbf{d}}}|^2 - \dot{\Delta} (1 + \Delta^2 \tau_2^2)}{1 + \Delta^2 \tau_2^2 + \tau_1 \tau_2 |\dot{\hat{\mathbf{d}}}|^2}. \end{aligned} \quad (\text{S19})$$

The first term leads to geometric dissipation (see Eq. (6) in the main text). The second term averages to zero over a period when the diabatic correction $\sim |\dot{\hat{\mathbf{d}}}|^2$ in the denominator can be neglected, as it can then be expressed as a total time derivative.

Finite-temperature extension

We now consider contributions to dissipation when the heat bath is at a non-zero temperature T_B . Assuming an isotropic dissipator, we have $\mathbf{S}_0 = -\tanh(\beta\Delta/2)\hat{\mathbf{d}}$ which points against the direction of the instantaneous Hamiltonian. Therefore, we simply need to solve a generalization of the Bloch equation in the rotating-frame basis, Eq. (S9), with $\mathbf{S}'_0 = -\tanh(\beta\Delta/2)\hat{\mathbf{z}}$:

$$\dot{\mathbf{S}}' = \left[\Delta \hat{\mathbf{z}} - R(\hat{\mathbf{d}} \times \dot{\hat{\mathbf{d}}}) \right] \times \mathbf{S}' - \Gamma' \left(\mathbf{S}' + \tanh \frac{\beta\Delta}{2} \hat{\mathbf{z}} \right). \quad (\text{S20})$$

Following the steps outlined above, we are interested in finding a solution to the above equation which is stationary to linear order in ω . One could naively attempt to generalize the arguments applied to the low-temperature limit, leading to $\mathbf{S}'_{\text{st}} = \mathbf{v}$, where $\mathbf{v} \equiv -\frac{M^{-1}}{\tau_1} \tanh(\beta\Delta/2)\hat{\mathbf{z}}$, with the M matrix given by Eq. (S17). Explicitly,

$$\mathbf{v} = \frac{\tanh(\beta\Delta/2)}{1 + \Delta^2\tau_2^2 + \tau_1\tau_2|\dot{\hat{\mathbf{d}}}|^2} \begin{pmatrix} |\dot{\hat{\mathbf{d}}}| \tau_2 \\ |\dot{\hat{\mathbf{d}}}| \Delta \tau_2^2 \\ -1 - \Delta^2\tau_2^2 \end{pmatrix}. \quad (\text{S21})$$

However, this solution does not constitute a legitimate solution to linear order in ω/Δ , because its time derivative $\dot{\mathbf{S}}_{\text{st}}$ contains a term linear in ω :

$$\dot{\mathbf{v}} = -\frac{\beta\dot{\Delta}/2}{\cosh^2(\beta\Delta/2)} \hat{\mathbf{z}} + \mathcal{O}\left(\frac{\omega^2}{\Delta}\right). \quad (\text{S22})$$

We thus need to perform one more step: solving Eq. (S20) with the left-hand side replaced by Eq. (S22) instead of set to zero. Doing this, we obtain the steady-state

$$\tilde{\mathbf{S}}'_{\text{st}} = -M^{-1} \left(\frac{\tanh(\beta\Delta/2)}{\tau_1} - \frac{\beta\dot{\Delta}/2}{\cosh^2(\beta\Delta/2)} \right) \hat{\mathbf{z}}, \quad (\text{S23})$$

Explicitly,

$$\tilde{\mathbf{S}}'_{\text{st}} = \frac{\left(\tanh(\beta\Delta/2) - \tau_1 \frac{\beta\dot{\Delta}/2}{\cosh^2(\beta\Delta/2)} \right)}{1 + \Delta^2\tau_2^2 + \tau_1\tau_2|\dot{\hat{\mathbf{d}}}|^2} \begin{pmatrix} |\dot{\hat{\mathbf{d}}}| \tau_2 \\ |\dot{\hat{\mathbf{d}}}| \Delta \tau_2^2 \\ -1 - \Delta^2\tau_2^2 \end{pmatrix}. \quad (\text{S24})$$

One can check that the Bloch equation Eq. (S20) is satisfied to linear-order in ω by inserting $\tilde{\mathbf{S}}'_{\text{st}}$ in Eq. (S24), thus providing a legitimate diabatic expansion.

Having found the steady-state solution in Eq. (S24), we next compute the dissipated power, obtaining

$$P_d = \frac{1}{2} \Delta \dot{\mathbf{d}} \cdot \mathbf{S}_{\text{st}} + \frac{1}{2} \dot{\Delta} \hat{\mathbf{d}} \cdot \mathbf{S}_{\text{st}} = \frac{\Delta |\dot{\mathbf{d}}|}{2} \hat{\mathbf{x}} \cdot \mathbf{S}'_{\text{st}} + \frac{\dot{\Delta}}{2} \hat{\mathbf{z}} \cdot \mathbf{S}'_{\text{st}} \quad (\text{S25})$$

$$= \frac{\tanh \frac{\beta \Delta}{2} \left(\Delta \tau_2 |\dot{\mathbf{d}}|^2 - \dot{\Delta} (1 + \Delta^2 \tau_2^2) \right) + \frac{\tau_1 \beta}{2 \cosh^2 \frac{\beta \Delta}{2}} \left(-\Delta \dot{\Delta} \tau_2 |\dot{\mathbf{d}}|^2 + \dot{\Delta}^2 (1 + \Delta^2 \tau_2^2) \right)}{2 \left(1 + \Delta^2 \tau_2^2 + \tau_1 \tau_2 |\dot{\mathbf{d}}|^2 \right)}. \quad (\text{S26})$$

First of all, we neglect the term that contains three time derivatives, as it is subleading in the adiabatic limit (where $\omega, 1/\tau_2 \ll \Delta$, see Fig. S1). Furthermore, if τ_1 and τ_2 are of the same order, we can also neglect the term $|\dot{\mathbf{d}}|^2$ term in the denominator. In this case, as also explained in the main text, the term proportional to $\dot{\Delta}$ vanishes, as it can be rewritten as a total time derivative. We then arrive at a much simpler expression for finite-temperature dissipation,

$$P_d = \frac{1}{2} \frac{\Delta \tau_2 \tanh \frac{\beta \Delta}{2}}{1 + \Delta^2 \tau_2^2} |\dot{\mathbf{d}}|^2 + \frac{\tau_1 \beta}{4 \cosh^2 \frac{\beta \Delta}{2}} \dot{\Delta}^2. \quad (\text{S27})$$

The first term above is simply the finite-temperature generalization of the quantum geometric dissipation discussed in the main text. The second term is intrinsically a finite-temperature dissipation effect that arises from the time-dependence of the gap magnitude Δ . This term depends linearly on the longitudinal relaxation time scale τ_1 , and is suppressed exponentially as $\beta e^{-\beta \Delta}$ at low temperatures.

GENERIC LOWER AND UPPER BOUNDS ON THE DISSIPATION

Here, we derive the lower bound on the dissipation away from the symmetric case and an upper bound. As follows from Eq. (11) in the main text, the average dissipation is given by

pation is given by

$$\bar{P}_d = \frac{1}{T} \int_0^T dt \gamma [\omega_1^2 g_{11} + \omega_2^2 g_{22} + 2\omega_1 \omega_2 g_{12}]. \quad (\text{S28})$$

For convenience, we parametrize, $\sqrt{g_{11}g_{22}} = r$, and $g_{12} = r \cos(\theta)$, using two parameters, $\theta = [-\pi, \pi]$ and r . From the definition of the Berry curvature, it follows $\Omega = 2r \sin(\theta)$. Next we use the inequality $2r \leq g_{11} + g_{22}$, and $2r \geq \Omega$, to find

$$\frac{|C|}{4\pi} \leq \iint \frac{d\phi_1 d\phi_2}{4\pi^2} r \leq \frac{\mathcal{P}_1 + \mathcal{P}_2}{2\Delta_{\text{min}}^2}, \quad (\text{S29})$$

where $\mathcal{P}_i = \iint \frac{d\phi_1 d\phi_2}{4\pi^2} (\partial_i \mathbf{d})^2$.

Lower bound

We begin with the lower bound, in this case we can use the inequality $\omega_1^2 g_{11} + \omega_2^2 g_{22} + 2\omega_1 \omega_2 g_{12} \geq 2\omega_1 \omega_2 r [1 + \cos(\theta)] \geq \omega_1 \omega_2 r [1 - \cos^2(\theta)] = \omega_1 \omega_2 r \sin^2(\theta)$. Therefore, using Eq. (S28), the bound on the dissipation reads

$$\bar{P}_d \geq \omega_1 \omega_2 \iint \frac{d\phi_1 d\phi_2}{4\pi^2} \gamma r \sin^2(\theta). \quad (\text{S30})$$

Next, we rewrite θ in terms of Ω , using the parametrization of Ω , to arrive at

$$\bar{P}_d \geq \omega_1 \omega_2 \iint \frac{d\phi_1 d\phi_2}{4\pi^2} \gamma \frac{\Omega^2}{4r}. \quad (\text{S31})$$

To make progress, we use the following sequence of inequalities, using the Cauchy-Schwarz inequality, to obtain

$$\frac{|C|}{2\pi} = \left| \iint \frac{d\phi_1 d\phi_2}{4\pi^2} \Omega \right| \leq \iint \frac{d\phi_1 d\phi_2}{4\pi^2} |\Omega| = \iint \frac{d\phi_1 d\phi_2}{4\pi^2} \frac{|\Omega| \sqrt{r}}{\sqrt{r}} \leq \sqrt{\iint \frac{d\phi_1 d\phi_2}{4\pi^2} \frac{\Omega^2}{r} \iint \frac{d\phi_1 d\phi_2}{4\pi^2} r}. \quad (\text{S32})$$

Rearranging and squaring the first and last terms of the inequality gives rise to

$$\iint \frac{d\phi_1 d\phi_2}{4\pi^2} \frac{\Omega^2}{r} \geq \frac{C^2}{4\pi^2 \iint \frac{d\phi_1 d\phi_2}{4\pi^2} r}. \quad (\text{S33})$$

Next, using the inequality in Eq. (S29), we obtain

$$\iint \frac{d\phi_1 d\phi_2}{4\pi^2} \frac{\Omega^2}{r} \geq \frac{\Delta_{\text{min}}^2 C^2}{2\pi^2 (\mathcal{P}_1 + \mathcal{P}_2)}. \quad (\text{S34})$$

Finally, using $\gamma \geq \gamma_{\text{min}}$ in Eq. (S31), taking γ_{min} outside the integral and using Eq. (S34), we arrive at the

lower bound on the dissipation,

$$\bar{P}_d \geq \frac{\omega_1 \omega_2 \gamma_{\min} \Delta_{\min}^2 \mathcal{C}^2}{8\pi^2 (\mathcal{P}_1 + \mathcal{P}_2)}. \quad (\text{S35})$$

Upper bound

Next, we proceed to find the upper bound on \bar{P}_d . Here, we use the inequality $g_{11}\omega_1^2 + g_{22}\omega_2^2 + 2g_{12}\omega_1\omega_2 \leq 2(g_{11}\omega_1^2 + g_{22}\omega_2^2)$.

Next, we use $\gamma \leq \gamma_{\max}$, and take γ_{\max} outside of the integral, to arrive at

$$\bar{P}_d \leq 2\gamma_{\max} \iint \frac{d\phi_1 d\phi_2}{4\pi^2} [g_{11}\omega_1^2 + g_{22}\omega_2^2]. \quad (\text{S36})$$

Next, we use an explicit expression $g_{11} = \frac{1}{\Delta^2} [(\partial_1 \mathbf{d})^2 - (\partial_1 \Delta)^2]$, to obtain $g_{11} \leq \frac{(\partial_1 \mathbf{d})^2}{\Delta_{\min}^2}$, and similarly for g_{22} , yielding the upper bound on the dissipation,

$$\bar{P}_d \leq 2\gamma_{\max} \frac{\omega_1^2 \mathcal{P}_1 + \omega_2^2 \mathcal{P}_2}{\Delta_{\min}^2}. \quad (\text{S37})$$

SYMMETRY CONDITIONS FOR VANISHING OF THE AVERAGED g_{12}

Here, we find the conditions on the symmetries of the system for $\int \frac{d\phi_1 d\phi_2}{4\pi^2} g_{12} = 0$. We consider a two-level system irradiated by two monochromatic drives, coupled to the spin trough

$$\mathbf{d} = \mathbf{B}_1(\phi_1) + \mathbf{B}_2(\phi_2) + \mathbf{m}, \quad (\text{S38})$$

where $\phi_i = \omega_i t$. We use the following definition of the quantum metric, which can be derived from $g_{ab} = \frac{1}{4} \partial_{\phi_a} \hat{\mathbf{d}} \cdot \partial_{\phi_b} \hat{\mathbf{d}}$, reading

$$g_{ab} = \frac{3}{16} \frac{\partial_{\phi_a} \partial_{\phi_b} d^2}{d^2} - \frac{1}{4} \frac{\mathbf{d} \cdot \partial_{\phi_a} \partial_{\phi_b} \mathbf{d}}{d^2} - \frac{1}{32} \frac{\partial_{\phi_a} \partial_{\phi_b} d^4}{d^4}, \quad (\text{S39})$$

where $d = |\mathbf{d}|$. For the form of \mathbf{d} in Eq. (S38), the second term in the RHS of g_{12} vanishes, $\partial_{\phi_1} \partial_{\phi_2} \mathbf{d} = 0$, giving rise to

$$g_{12} = \frac{3}{16} \frac{\partial_{\phi_1} \partial_{\phi_2} d^2}{d^2} - \frac{1}{32} \frac{\partial_{\phi_1} \partial_{\phi_2} d^4}{d^4}, \quad (\text{S40})$$

which is only expressed in terms of the scalar $d^2 = \mathbf{B}_1^2(\phi_1) + \mathbf{B}_2^2(\phi_2) + \mathbf{m}^2 + 2\mathbf{B}_1(\phi_1) \cdot \mathbf{B}_2(\phi_2) + 2\mathbf{B}_1(\phi_1) \cdot \mathbf{m} + 2\mathbf{B}_2(\phi_2) \cdot \mathbf{m}$.

We are interested in finding the symmetry conditions that enforce that g_{12} in Eq. (S40) averages to zero when averaging over the phases ϕ_1 and ϕ_2 . For this to occur, the norm d^2 should be even under reversal of either one of the phases, $\phi_a \rightarrow -\phi_a + c$ with $a = 1$ or 2 and c a constant. Then, the corresponding derivative ∂_{ϕ_a} ensures

that g_{12} is an odd function over the period of ϕ_a , and the integral therefore vanishes. Here, we will require g_{12} to be odd in ϕ_1 .

We consider a generic situation where both drives are elliptically polarized with arbitrary orientations in three dimensions,

$$\mathbf{B}_1(\phi_1) = b_{1,e}(\phi_1) \hat{\mathbf{e}}_1 + b_{1,o}(\phi_1) \hat{\mathbf{e}}_2, \quad (\text{S41})$$

$$\mathbf{B}_2(\phi_2) = b_{2,e}(\phi_2) \hat{\mathbf{e}}_3 + b_{2,o}(\phi_2) \hat{\mathbf{e}}_4. \quad (\text{S42})$$

where the principal axes of the two ellipses are respectively orthogonal, $\hat{\mathbf{e}}_1 \perp \hat{\mathbf{e}}_2$ and $\hat{\mathbf{e}}_3 \perp \hat{\mathbf{e}}_4$. Without loss of generality, we choose the origin of time such that the functions $b_{a,e}$ and $b_{a,o}$ are respectively even and odd under $\phi_a \rightarrow -\phi_a$ (in other words, at $\phi_1 = 0$ the polarization vector lies along $\hat{\mathbf{e}}_1$). Therefore we have $\mathbf{B}_a^2(\phi_a) = b_{a,e}^2(\phi_a) + b_{a,o}^2(\phi_a)$ which is even under reversing ϕ_a . There are two non-trivial terms that impose conditions on the driving protocol:

$$\begin{aligned} \mathbf{B}_1 \cdot \mathbf{B}_2 &= b_{1,e}(\phi_1) b_{2,e}(\phi_2) \hat{\mathbf{e}}_1 \cdot \hat{\mathbf{e}}_3 + b_{1,e}(\phi_1) b_{2,o}(\phi_2) \hat{\mathbf{e}}_1 \cdot \hat{\mathbf{e}}_4 \\ &\quad + b_{1,o}(\phi_1) b_{2,e}(\phi_2) \hat{\mathbf{e}}_2 \cdot \hat{\mathbf{e}}_3 + b_{1,o}(\phi_1) b_{2,o}(\phi_2) \hat{\mathbf{e}}_2 \cdot \hat{\mathbf{e}}_4 \end{aligned} \quad (\text{S43})$$

and

$$\mathbf{B}_1 \cdot \mathbf{m} = b_{1,e}(\phi_1) \hat{\mathbf{e}}_1 \cdot \mathbf{m} + b_{1,o}(\phi_1) \hat{\mathbf{e}}_2 \cdot \mathbf{m}. \quad (\text{S44})$$

We want both functions to be even under ϕ_1 . This requires that the odd contribution, $b_{1,o}$, vanishes. To this end, we require $\hat{\mathbf{e}}_2 \perp \hat{\mathbf{e}}_3, \hat{\mathbf{e}}_4$ in Eq. (S43). The two drives, therefore, form a right-angle triad of vectors (remember that also $\hat{\mathbf{e}}_3 \perp \hat{\mathbf{e}}_4$ due to their being the principal axes of an ellipse.) Alternatively, that corresponds to $\mathbf{S}_1 \perp \mathbf{S}_2$, where $\mathbf{S}_a = \mathbf{B}_a \times \partial_{\phi_a} \mathbf{B}_a$ is the angular momentum of the drive. In addition, Eq. (S44) leads to a condition on the relative orientation of the mass term and the drive, $\hat{\mathbf{e}}_2 \perp \mathbf{m}$. Because \mathbf{S}_2 is parallel to $\hat{\mathbf{e}}_2$ this condition is equivalent to $\mathbf{S}_2 \perp \mathbf{m}$.

The argument above can be run using ϕ_2 instead. The condition on the relative angular momentum vectors of the two drives being perpendicular remains unchanged, whereas the condition that invokes the mass term becomes instead $\hat{\mathbf{S}}_1 \perp \mathbf{m}$. Because only one of the ϕ_a integrals needs to vanish, either condition is sufficient. In summary, if $\mathbf{S}_1 \perp \mathbf{S}_2$ and either $\mathbf{S}_1 \perp \mathbf{M}$ or $\mathbf{S}_2 \perp \mathbf{M}$, the phase-average of g_{12} will vanish.

DISSIPATION IN A SYSTEM WITH AN ARBITRARY NUMBER OF BANDS

Here, we find the energy dissipation rate for an arbitrary number of bands of (non-degenerate) bands, generalizing Eq. (8) in the main text. We start from the master equation which reads (dropping explicit dependence on t),

$$\dot{\rho} = -i[H, \rho] + \mathcal{D}\{\rho\}. \quad (\text{S45})$$

Next, we transform Eq. (S45) to the instantaneous diagonal basis of H by applying a unitary transformation U . Such that $UHU^\dagger = H_d$, where H_d is diagonal and $\rho_d = U\rho U^\dagger$, leading to

$$\dot{\rho}_d = -i[H_d + \mathcal{A}^i \dot{\alpha}^i, \rho_d] + \mathcal{D}'\{\rho_d\}, \quad (\text{S46})$$

where $\mathcal{A}^i \dot{\alpha}^i = i\dot{U}U^\dagger$, denotes the Berry connection tensor $\mathcal{A}_{mn}^i(\boldsymbol{\alpha}) = -i\langle \psi_m(\boldsymbol{\alpha}) | \partial_{\alpha^i} | \psi_n(\boldsymbol{\alpha}) \rangle$ for bands labeled by m, n , and $\mathcal{D}' = U\mathcal{D}U^\dagger$, with $|\psi_m(\boldsymbol{\alpha})\rangle$ the m th eigenstate of $H(\boldsymbol{\alpha})$. (Here the index i denotes a spatial component.) We consider the full density matrix ρ_d , written in the instantaneous eigenbasis of H as

$$\rho_{mn} = \rho_m^{\text{eq}} \delta_{mn} + \delta\rho_{mn}. \quad (\text{S47})$$

(Throughout, we suppress the index “ d ” for the elements of ρ .) The diagonal contributions ρ_m^{eq} for each band denote their corresponding equilibrium values, whereas $\delta\rho_{mn}$ denote the diabatic corrections. The form of the dissipator is chosen as a generalization of the main text expression, Eq. (4),

$$\mathcal{D}'\{\rho\}_{mn} = -\delta\rho_{mn}/\tau_{mn}. \quad (\text{S48})$$

where τ_{mn} denotes the inter-band relaxation timescale associated with transitions between bands m and n . This form of the dissipator can be derived from first principles in the limit of slow driving, provided that the relaxation rate is much smaller than any spectral gap of the system [2].

We now evaluate the commutator $C = [H_d + \mathcal{A}^i \dot{\alpha}^i, \rho]$ in Eq. (S46). It is helpful to separate C in diagonal and off-diagonal components. The diagonal components read

$$\begin{aligned} C_{mm} &= \sum_{p \neq m} \left[(H_d + \mathcal{A}^i \dot{\alpha}^i)_{mp} \rho_{pm} - \rho_{mp} (H_d + \mathcal{A}^i \dot{\alpha}^i)_{pm} \right] \\ &= \sum_{p \neq m} [\mathcal{A}_{mp}^i \rho_{pm} - \rho_{mp} \mathcal{A}_{pm}^i] \dot{\alpha}^i \end{aligned} \quad (\text{S49})$$

where the contributions with $p = m$ vanish trivially. The off-diagonal contributions (with $m \neq n$) read

$$\begin{aligned} C_{mn} &= \sum_p \left[(H_d + \mathcal{A}^i \dot{\alpha}^i)_{mp} \rho_{pn} - \rho_{mp} (H_d + \mathcal{A}^i \dot{\alpha}^i)_{pn} \right] \\ &= \sum_{p \neq m, n} [\mathcal{A}_{mp}^i \rho_{pn} - \rho_{mp} \mathcal{A}_{pn}^i] \dot{\alpha}^i + \mathcal{A}_{mn}^i \dot{\alpha}^i (\rho_{nn} - \rho_{mm}) \\ &\quad + (E_m + \mathcal{A}_{mm}^i \dot{\alpha}^i - E_n - \mathcal{A}_{nn}^i \dot{\alpha}^i) \rho_{mn}, \end{aligned} \quad (\text{S50})$$

where E_m is the energy of the level m . Taking $\dot{\rho} = 0$ to find steady-state solutions to the master equation leads to a separate condition for each of its components. First consider the off-diagonal ones:

$$0 = -iC_{mn} - \frac{\delta\rho_{mn}}{\tau_{mn}} \quad (\text{S51})$$

Solving for the diabatic correction $\delta\rho_{mn}$,

$$\delta\rho_{mn} = \frac{\mathcal{A}_{mn}^i \dot{\alpha}^i (\rho_n^{\text{eq}} - \rho_m^{\text{eq}}) + \sum_p [\mathcal{A}_{mp}^i \delta\rho_{pn} - \delta\rho_{mp} \mathcal{A}_{pn}^i] \dot{\alpha}^i}{E_m + \mathcal{A}_{mm}^i \dot{\alpha}^i - E_n - \mathcal{A}_{nn}^i \dot{\alpha}^i - i/\tau_{mn}}, \quad (\text{S52})$$

where the sum is over $p \neq m, n$. To leading-order the terms in the sum can be neglected because they contain additional factors of $\dot{\alpha}^i$ coming from off-diagonal contributions to ρ from other transition to other bands p . Similarly, the contribution from the quantum geometric potential in the denominator can be neglected as it produces a contribution quadratic in $\dot{\alpha}^i$. We thus have

$$\delta\rho_{mn} = \frac{\mathcal{A}_{mn}^i \dot{\alpha}^i (\rho_m^{\text{eq}} - \rho_n^{\text{eq}})}{E_m - E_n - i/\tau_{mn}}. \quad (\text{S53})$$

Similarly, the diagonal components read

$$\begin{aligned} \delta\rho_{mm} &= -i\tau_{mm} \sum_{p \neq m} [\mathcal{A}_{mp}^i \delta\rho_{pm} - \delta\rho_{mp} \mathcal{A}_{pm}^i] \dot{\alpha}^i \\ &= 2\tau_{mm} \sum_{p \neq m} \text{Im} [\mathcal{A}_{mp}^i \delta\rho_{pm}] \dot{\alpha}^i. \end{aligned} \quad (\text{S54})$$

Notice that we focused on a zero temperature case, in which $\rho^{\text{eq}} = 0$. It follows from Eq. (S54) that the diagonal components are of higher order in the diabatic expansion, and thus can be neglected.

The average dissipation rate is given by $\bar{P}_d = \frac{1}{T} \int_0^T dt \text{Tr}[\dot{H}\rho]$. On a diagonal basis, the dissipation reads

$$\bar{P}_d = \frac{1}{T} \int_0^T dt \text{Tr} \{ -i[H_d, \mathcal{A}^i \dot{\alpha}^i] \rho_d + \dot{H}_d \rho_d \}. \quad (\text{S55})$$

The commutator in the trace can be explicitly evaluated, resulting in a purely off-diagonal matrix $[H_d, \mathcal{A}^i \dot{\alpha}^i]_{mn} = \mathcal{A}_{mn}^i \dot{\alpha}^i (E_m - E_n)$. To continue, we use the expansion of ρ_d in Eq. (S47). The term proportional to ρ^{eq} vanishes under the time average. Therefore, we need to use the second term $\delta\rho_d$ up to linear order in $\dot{\alpha}$. As we found in Eqs. (S53) and (S54), this order only appears in the off-diagonal elements of $\delta\rho_d$. Therefore, only the term proportional to a commutator in Eq. (S55) remains, yielding

$$\bar{P}_d = \frac{1}{T} \int_0^T dt \Lambda_{ij}^{(N)} \dot{\alpha}^i \dot{\alpha}^j \quad \text{where} \quad \Lambda_{ij}^{(N)} = -i \sum_{m \neq n} (\rho_m^{\text{eq}} - \rho_n^{\text{eq}}) \frac{\mathcal{A}_{mn}^i \mathcal{A}_{nm}^j}{1 + i/\Delta_{mn} \tau_{mn}}. \quad (\text{S56})$$

Here we used that $\tau_{nm} = \tau_{mn}$ and defined the spectral gap $\Delta_{mn} = E_m - E_n$. Equivalently, we can obtain a convenient expression for the metric by writing the sum as

$$\begin{aligned}\Lambda_{ij}^{(N)} &= -i \sum_{m < n} (\rho_m^{\text{eq}} - \rho_n^{\text{eq}}) \left\{ \frac{\mathcal{A}_{mn}^i \mathcal{A}_{nm}^j}{1 + i/\Delta_{mn}\tau_{mn}} - \frac{\mathcal{A}_{nm}^i \mathcal{A}_{mn}^j}{1 - i/\Delta_{mn}\tau_{mn}} \right\} \\ &= 2 \sum_{m < n} (\rho_n^{\text{eq}} - \rho_m^{\text{eq}}) \text{Im} \left\{ \frac{\mathcal{A}_{mn}^i \mathcal{A}_{nm}^j}{1 + i/\Delta_{mn}\tau_{mn}} \right\}.\end{aligned}\quad (\text{S57})$$

Contrary to the two-level version, the expression inside the bracket cannot be identified with the quantum geometric tensor for band m .

In the low-temperature limit, where only the ground-state energy level is occupied in the instantaneous equilibrium state ($\rho_0^{\text{eq}} = 1$ and $\rho_{m \neq 0}^{\text{eq}} = 0$), the above expression simplifies to

$$\Lambda_{ij}^{(N)} = -2 \sum_{n \neq 0} \text{Im} \left\{ \frac{\mathcal{A}_{0n}^i \mathcal{A}_{n0}^j}{1 + i/\Delta_{0n}\tau_{0n}} \right\}, \quad (\text{S58})$$

which can be rewritten as

$$\Lambda_{ij}^{(N)} = 2 \sum_{n \neq 0} \frac{\mathcal{A}_{0n}^i \mathcal{A}_{n0}^j}{\Delta_{0n}\tau_{0n} + \Delta_{0n}^{-1}\tau_{0n}^{-1}}. \quad (\text{S59})$$

This is a positive semidefinite matrix, since for any real vector \mathbf{v} ,

$$\mathbf{v}^T \Lambda^{(N)} \mathbf{v} = 2 \sum_{n \neq 0} \frac{|v_{0n}|^2}{\Delta_{0n}\tau_{0n} + \Delta_{0n}^{-1}\tau_{0n}^{-1}} \geq 0 \quad (\text{S60})$$

where $v_{0n} = \sum_i \mathcal{A}_{0n}^i v_i$ and we exploited $\mathcal{A}_{0n}^i = (\mathcal{A}_{n0}^i)^*$.

We establish the bound quoted in the main text using the identity $1 \geq \frac{2}{\Delta_{0n}\tau_{0n} + \Delta_{0n}^{-1}\tau_{0n}^{-1}} \geq \gamma^{(N)}$, where

$$\gamma^{(N)} = \min_n \frac{2}{\Delta_{0n}\tau_{0n} + \Delta_{0n}^{-1}\tau_{0n}^{-1}}. \quad (\text{S61})$$

This leads to

$$G^{(N)} \succeq \Lambda^{(N)} \succeq \gamma^{(N)} G^{(N)}, \quad (\text{S62})$$

as quoted in Eq. (10) of the main text, where

$$G_{ij}^{(N)} = \sum_n \mathcal{A}_{0n}^i \mathcal{A}_{n0}^j = \frac{1}{2} \text{Tr}[\partial_{\alpha^i} P_0 \partial_{\alpha^j} P_0] \quad (\text{S63})$$

is the ground state quantum metric, and P_0 denotes a ground-state projector. Here the inequality \succeq between metrics A and B should be understood such that $A \succeq B$ if and only if $\mathbf{v}^T A \mathbf{v} \geq \mathbf{v}^T B \mathbf{v} \geq 0$ for all real-valued vectors \mathbf{v} . The resulting inequality translates directly to a corresponding inequality for the energy dissipation.

DERIVATION OF THE MASTER EQUATION FROM A MICROSCOPIC MODEL

Here we derive the master equation appearing in Eq. (3) in the main text from a microscopic model. We consider a cloud of $N_c + 1$ spins coupled to a time-dependent magnetic field described by the Hamiltonian

$$H = \sum_{i=0}^{N_c} \mathbf{d}_0(t) \cdot \boldsymbol{\sigma}_i + \sum_{i>j} J_{ij} \boldsymbol{\sigma}_i \cdot \boldsymbol{\sigma}_j. \quad (\text{S64})$$

We assume a weakly coupled cloud, with $\sum_j |J_{ij}| \ll |\mathbf{d}_0|$, such that the spins are approximately aligned with $-\mathbf{d}_0(t)$ at any time, up to small fluctuations. Without loss of generality, we focus on a single spin with $i = 0$ treating it as a system and treating the rest of the spins as a heat bath. For simplicity, we rewrite H as $H = H_0 + H_{\text{int}} + H_B$, where

$$H_0 = \mathbf{d}(t) \cdot \boldsymbol{\sigma}_0, \quad H_{\text{int}} = \sum_i J_{0i} \boldsymbol{\sigma}_0 \cdot \delta \boldsymbol{\sigma}_i \quad (\text{S65})$$

with $\delta \boldsymbol{\sigma}_i = \boldsymbol{\sigma}_i + \hat{\mathbf{d}}_0(t)$, $\mathbf{d}(t) = \hat{\mathbf{d}}_0(t)(d - \sum_i J_{0i})$, and $H_B(t)$ denotes all the terms which are independent of $\boldsymbol{\sigma}_0$, i.e., describes the dynamics of the rest of the spins $\boldsymbol{\sigma}_i$, for $i > 0$.

The kinetic equation describing the dynamics of the total density matrix of the system in the interaction picture, $\tilde{\rho}$, reads [1]

$$\partial_t \tilde{\rho}(t) = - \int_0^t dt' [\tilde{H}_{\text{int}}(t), [\tilde{H}_{\text{int}}(t'), \tilde{\rho}(t')]], \quad (\text{S66})$$

where $\tilde{H}_{\text{int}}(t) = \hat{U}_B^\dagger(t) \hat{U}_0^\dagger(t) H_{\text{int}} \hat{U}_0(t) \hat{U}_B(t)$ is the interaction picture representation of H_{int} , and

$$\hat{U}_0(t) = \mathcal{T} e^{-i \int_0^t dt' H_0(t')}, \quad \hat{U}_B(t) = \mathcal{T} e^{-i \int_0^t dt' H_B(t')} \quad (\text{S67})$$

are the time evolution operators of the $i = 0$ spin and the rest of the spins. We also define $\tilde{\boldsymbol{\sigma}}_i(t) = \hat{U}_B^\dagger(t) \hat{U}_0^\dagger(t) \boldsymbol{\sigma}_i \hat{U}_0(t) \hat{U}_B(t)$ to denote spins in the interaction picture.

Next, we focus on a single spin $\tilde{\boldsymbol{\sigma}}_0$, described by a reduced density matrix $\tilde{\rho}_0$, and assume the rest of the spins, described by the density matrix $\tilde{\rho}_B$, as its heat bath. This heat bath essentially describes vibrational modes of the cloud around an instantaneous ferromagnetic state, in which all the spins are pointing along $-\mathbf{d}_0(t)$.

The correlation time τ_c of the vibrations decays with J_{ij} . Here, we consider the limit, $\omega\tau_c \ll 1$, in which the vibrational modes thermalize much faster than the change in $\mathbf{d}_0(t)$. Under these conditions, the heat bath can be assumed in the instantaneous thermal equilibrium.

Furthermore, for large N_c , we assume that $\tilde{\rho}_B$ is approximately unaffected by the interaction with $\tilde{\sigma}_0$, therefore, we can write $\tilde{\rho}(t) = \tilde{\rho}_0(t) \otimes \tilde{\rho}_B(t)$. Separating Eq. (S66) to components dependent on $\tilde{\sigma}_0$ and the heat bath, we arrive at

$$\begin{aligned} \partial_t \tilde{\rho}(t) = & - \sum_{ij} J_{0i} J_{0j} \int_0^t dt' [\tilde{\sigma}_0^\alpha(t) \tilde{\sigma}_0^\beta(t') \tilde{\rho}_0(t') \delta \tilde{\sigma}_i^\alpha(t) \delta \tilde{\sigma}_j^\beta(t') \tilde{\rho}_B(t') + \tilde{\rho}_0(t') \tilde{\sigma}_0^\beta(t') \tilde{\sigma}_0^\alpha(t) \tilde{\rho}_B(t') \delta \tilde{\sigma}_j^\beta(t') \delta \tilde{\sigma}_i^\alpha(t) - \\ & - \tilde{\sigma}_0^\beta(t') \tilde{\rho}_0(t') \tilde{\sigma}_0^\alpha(t) \delta \tilde{\sigma}_j^\beta(t') \tilde{\rho}_B(t') \delta \tilde{\sigma}_i^\alpha(t) - \tilde{\sigma}_0^\alpha(t) \tilde{\rho}_0(t') \tilde{\sigma}_0^\beta(t') \delta \tilde{\sigma}_i^\alpha(t) \tilde{\rho}_B(t') \delta \tilde{\sigma}_j^\beta(t')], \end{aligned} \quad (\text{S68})$$

where $\alpha, \beta = x, y, z$. Next, we trace over the degrees of freedom of the heat bath, arriving at

$$\begin{aligned} \partial_t \tilde{\rho}_0(t) = & - \sum_{ij} J_{0i} J_{0j} \int_0^t dt' [(\tilde{\sigma}_0^\alpha(t) \tilde{\sigma}_0^\beta(t') \tilde{\rho}_0(t') - \tilde{\sigma}_0^\beta(t') \tilde{\rho}_0(t') \tilde{\sigma}_0^\alpha(t)) \chi_{ij}^{>, \alpha\beta}(t, t') + \\ & + (\tilde{\rho}_0(t') \tilde{\sigma}_0^\beta(t') \tilde{\sigma}_0^\alpha(t) - \tilde{\sigma}_0^\alpha(t) \tilde{\rho}_0(t') \tilde{\sigma}_0^\beta(t')) \chi_{ij}^{<, \alpha\beta}(t, t')], \end{aligned} \quad (\text{S69})$$

where

$$\chi_{ij}^{>, \alpha\beta}(t, t') = \text{Tr}_B \{ \delta \tilde{\sigma}_i^\alpha(t) \delta \tilde{\sigma}_j^\beta(t') \tilde{\rho}_B(t') \}, \quad (\text{S70})$$

$$\chi_{ij}^{<, \alpha\beta}(t, t') = \text{Tr}_B \{ \delta \tilde{\sigma}_j^\beta(t') \delta \tilde{\sigma}_i^\alpha(t) \tilde{\rho}_B(t') \}, \quad (\text{S71})$$

are components of the spin correlation function of the heat bath.

To make progress, we use the Markov approximation setting $\tilde{\rho}_0(t') \approx \tilde{\rho}_0(t)$, which is valid in the regime $\lambda\tau_c \ll 1$, where λ is the characteristic rate of change of $\tilde{\rho}_0$, see below. Then we transform Eq. (S69) to the original basis by multiplying by $\hat{U}_0(t)$ from the left and $\hat{U}_0^\dagger(t)$ from the right. At this stage, we need to calculate $\hat{U}_0(t) \tilde{\sigma}_0^\alpha(t') \hat{U}_0^\dagger(t)$, which we do by expanding the evolution operator in the eigenbasis of $H_0(t)$, using $\hat{U}_0(t) = \sum_n e^{-i\varepsilon_n t} |n(t)\rangle \langle n|$, where $|n(t)\rangle$ is the n -th eigenstate of $H_0(t)$ for $n = \pm$ at time t and $|n\rangle$ is the same eigenstate at time $t = 0$; ε_n denotes the corresponding eigenenergy. An explicit calculation yields

$$\hat{U}_0(t) \tilde{\sigma}_0^\alpha(t') \hat{U}_0^\dagger(t) = \sum_{mn} e^{-i(\varepsilon_m - \varepsilon_n)(t-t')} \sigma_{0,mn}^\alpha |m\rangle \langle n|, \quad (\text{S72})$$

where $\sigma_{0,mn}^\alpha = \langle m | \sigma_0^\alpha | n \rangle$, and we used $\langle m(t) | n(t') \rangle \approx \delta_{mn}$ up to corrections of the order of $\sim \mathcal{O}(\omega\tau_c)$. After the transformation, Eq. (S69) reads

$$\begin{aligned} \partial_t \rho_0(t) + i[H_0(t), \rho_0(t)] = & \\ - \lambda_{mn}^{>, \alpha\beta} (\sigma_0^\alpha \sigma_{0,mn}^\beta \rho_0(t) - \sigma_{0,mn}^\beta \rho_0(t) \sigma_0^\alpha) & \\ - \lambda_{mn}^{<, \alpha\beta} (\rho_0(t) \sigma_{0,mn}^\beta \sigma_0^\alpha - \sigma_0^\alpha \rho_0(t) \sigma_{0,mn}^\beta), & \end{aligned} \quad (\text{S73})$$

where

$$\lambda_{mn}^{\gtrless, \alpha\beta}(t) = \sum_{ij} J_{0i} J_{0j} \int_0^t dt' e^{-i(\varepsilon_m - \varepsilon_n)(t-t')} \tilde{\chi}_{ij}^{\gtrless, \alpha\beta}(t, t'). \quad (\text{S74})$$

Finally, we transform Eq. (S73) to the instantaneous basis of $H_0(t)$, using the transformation unitary $\hat{U}_I(t)$, such that

$$\hat{U}_I^\dagger(t) \sigma_i^\alpha \hat{U}_I(t) = \check{\sigma}_i^\alpha(t) \quad (\text{S75})$$

$$\hat{U}_I^\dagger(t) \rho_i(t) \hat{U}_I(t) = \check{\rho}_i(t). \quad (\text{S76})$$

In the low-temperature and weak interaction limit, $\Delta \gg \sum_i |J_{ij}|$ and $\Delta \gg T$, $\langle \sigma_i(t) \rangle \approx -\hat{\mathbf{d}}(t)$ or alternatively $\langle \check{\sigma}_i(t) \rangle \approx -\hat{\mathbf{z}}$, up to corrections $\sim \mathcal{O}(J_{ij}/\Delta)$, $\sim \mathcal{O}(\omega/\Delta)$, and $\sim \mathcal{O}(T/\Delta)$, where Δ is the instantaneous gap of $H_0(t)$. In this regime, $\chi_{ij}^{>, +-}(t, t')$ is only non-zero for $\alpha = +$ and $\beta = -$, up to quadratic order corrections in small parameters. Similarly, $\chi_{ij}^{<, +-}(t, t')$ is also non-zero and the rest of the correlations can be neglected. We define

$$\chi_{ij}^{\alpha\beta}(\Delta t, \bar{t}) = \chi_{ij}^{\alpha\beta}(\bar{t} + \frac{1}{2}\Delta t, \bar{t} - \frac{1}{2}\Delta t), \quad (\text{S77})$$

where $\Delta t = t - t'$ defines the fast scale proportional to τ_c and $\bar{t} = (t + t')/2$ defines the slow scale proportional to ω . In the regime of local equilibrium, $\omega\tau_c \ll 1$, the two scales separate, and we can further approximate $\bar{t} \approx t$. Under the assumption of local equilibrium, the Fourier transformed correlation function, $\tilde{\chi}_{ij}^{\alpha\beta}(\Omega, t) = \int_{-\infty}^{\infty} d\Delta t e^{-i\Omega\Delta t} \chi_{ij}^{\alpha\beta}(\Delta t, t)$ is at thermal equilibrium at any t , satisfying $\tilde{\chi}_{ij}^{>, +-}(\Omega, t) = \tilde{\chi}_{ji}^{<, +-}(-\Omega, t)$.

Finally, the r.h.s. of Eq. (S73) can be written as

$$\lambda [2\check{\sigma}_0^- \check{\rho}_0(t) \check{\sigma}_0^+ - \check{\sigma}_0^+ \check{\sigma}_0^- \check{\rho}_0(t) - \check{\rho}_0(t) \check{\sigma}_0^+ \check{\sigma}_0^-], \quad (\text{S78})$$

where $\lambda = \sum_{ij} J_{0i} J_{0j} \tilde{\chi}_{ij}^{>, +-}(\Delta, t)$, and we neglected the Lamb-shift term for simplicity. The expression in Eq. (S78) vanishes for $\check{\rho}_0 = \check{\rho}_{\text{eq}} = \begin{pmatrix} 0 & 0 \\ 0 & 1 \end{pmatrix}$. Expanding $\check{\rho}_0$

to the linear order in $\delta\check{\rho} = \check{\rho}_0 - \check{\rho}_{\text{eq}}$, Eq. (S78) transforms to

$$- \begin{pmatrix} \frac{\delta\check{\rho}_{11}}{\tau_1} & \frac{\delta\check{\rho}_{12}}{\tau_2} \\ \frac{\delta\check{\rho}_{21}}{\tau_2} & \frac{\delta\check{\rho}_{22}}{\tau_1} \end{pmatrix}, \quad (\text{S79})$$

where $\tau_1^{-1} = 2\tau_2^{-1} = 2\lambda$, and $\delta\check{\rho}_{ij}$ are different compo-

nents of $\delta\check{\rho}$.

-
- [1] H.-P. Breuer, F. Petruccione, H.-P. Breuer, and F. Petruccione, The Theory of Open Quantum Systems (Oxford University Press, Oxford, New York, 2007).
- [2] G. D. Meglio, M. B. Plenio, and S. F. Huelga, [Time dependent markovian master equation beyond the adiabatic limit](#) (2023), [arXiv:2304.06166 \[quant-ph\]](#).